Journal Pre-proof

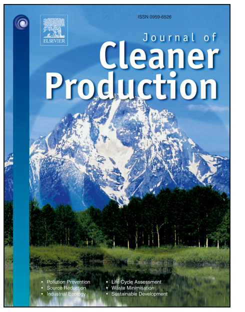

Spatial Differentiation and Driving Mechanisms in Ecosystem Service Value of Arid Region：A case study in the middle and lower reaches of Shule River Basin, NW China

Ninghui Pan, Qingyu Guan, Qingzheng Wang, Yunfan Sun, Huichun Li, Yunrui Ma

PII: S0959-6526(21)02917-6

DOI: https://doi.org/10.1016/j.jclepro.2021.128718

Reference: JCLP 128718

To appear in: *Journal of Cleaner Production*

Received Date: 26 February 2021

Revised Date: 28 July 2021

Accepted Date: 18 August 2021

Please cite this article as: Pan N, Guan Q, Wang Q, Sun Y, Li H, Ma Y, Spatial Differentiation and Driving Mechanisms in Ecosystem Service Value of Arid Region：A case study in the middle and lower reaches of Shule River Basin, NW China, *Journal of Cleaner Production* (2021), doi: https://doi.org/10.1016/j.jclepro.2021.128718.

Credit author statement

Ninghui Pan: Conceptualization, Methodology, Software, Data collection, curation and analysis, Formal analysis, Writing - original draft;

Qingyu Guan: Writing - review & editing, Supervision, Project administration, Funding acquisition;

Qingzheng Wang: Visualization, Validation, Data curation;

Yunfan Sun: Resources; Software;

Huichun Li: Software;

Yunrui Ma: Investigation

Spatial Differentiation and Driving Mechanisms in Ecosystem Service Value of Arid Region：A case study in the middle and lower reaches of Shule River Basin, NW China

Ninghui Pan, Qingyu Guan [*], Qingzheng Wang, Yunfan Sun, Huichun Li, Yunrui Ma

(Gansu Key Laboratory for Environmental Pollution Prediction and Control, College of Earth and Environmental Sciences, Lanzhou University, Lanzhou, 730000, China)

[*] Corresponding author: guanqy@lzu.edu.cn

Spatial Differentiation and Driving Mechanisms in Ecosystem Service Value of Arid Region：A case study in the middle and lower reaches of Shule River Basin, NW China

Ninghui Pan, Qingyu Guan [*], Qingzheng Wang, Yunfan Sun, Huichun Li, Yunrui Ma

(Gansu Key Laboratory for Environmental Pollution Prediction and Control, College of Earth and Environmental Sciences, Lanzhou University, Lanzhou, 730000, China)

Abstract: The determination of spatiotemporal variation in ecosystem service value and its drivers is fundamental to ecosystem service management and decision-making. This paper selects a typical oasis irrigation district in the arid regions of northwest China as the research object. Using the benefit transfer method to evaluate the ecosystem service value variation caused by land use and land cover change and characteristics of its spatial distribution based on multi-temporal land use and land cover data sets (1977, 1987, 1997, 2007, 2017). Meanwhile, the contributions of factors driving ecosystem service value and their interactions were explored using geographical detector. The results showed the following: 1) The land use and land cover structure was stable from 1977 to 2017, and the overall ecosystem service value increased slightly. The services provided by the oasis ecosystem dominated the fluctuations in ecosystem service value throughout the study region. 2) Ecosystem service value exhibited a strong positive spatial autocorrelation. The high values were concentrated in the oasis area in the north of the study area, while the low values mainly appeared in the desert ecosystem. 3) The land use degree and human activity intensity index of human factors are the main factors leading to the differentiation of ecosystem service value. Synergized interactions among human activities, changes in landscape

[*] Corresponding author: guanqy@lzu.edu.cn

patterns, and natural factors produced the spatial differentiation in ecosystem service value of the study region. The results suggest that in future decision-making for ecosystem management, the direction of human activities within the ecological environment should be controlled. Improve the diversity of patches, reduce the degree of landscape fragmentation, improve the ecosystem service function of LULC, optimize the allocation of ecological landscape resources.

Keywords: Land use and land cover change; Ecosystem service value; Spatiotemporal differentiation; Driving factors; Oasis-irrigated agricultural areas

1. Introduction

Land use/land cover (LULC) is an important tool for investigating the interaction of human activities with natural ecological environments. Changes in LULC directly affect the structure and function of an ecosystem (Kareiva and Wennergren, 1995; Lindenmayer and Franklin, 2010; Liu et al., 2012; Zhang et al., 2015; Rukundo et al., 2018; Peters et al., 2019; Wu et al., 2020). The International Geosphere-Biosphere Programme (IGBP) states that changes in the status, characteristics, and functions of ecosystems inevitably affect the supply of ecosystem services and cause changes in ecosystem service value (ESV) (Polasky et al., 2011; Hao et al., 2016; Song and Deng, 2017; Zhang et al., 2020b). Therefore, the scientific assessment of ESV, the construction of eco-security models, and the optimization of land use have become necessities for land-use planning and regional ecological security management (Xu et al., 2016; Wang et al., 2017; Kim et al., 2018; Mahmoud et al., 2018; Ma et al., 2019; Talukdar et al., 2020). A milestone in ESV assessment was the calculation of the equivalent ESV coefficient of the world, by Costanza et al.

(1997) (Song and Deng, 2017; Wang et al., 2018; Zhang et al., 2020b). Chinese scholar Xie et al. (2003), referring to part of the research results of Costanza et al. (1997), formulated the table of ecological service value equivalent factor of China's terrestrial ecosystem according to the reality of China through expert consultation. The Millennium Ecosystem Assessment (MEA) classifies ecosystem services into 4 major categories: provisioning, regulatory, support, and cultural services, and quantifying the importance of ecosystems to human well-being as one of its key goals (MEA, 2005). It is pointed out that the realization of this goal will be helpful for decision makers to formulate better strategies for sustainable utilization and management of ecosystem services. Later, scholars gradually incorporated the evaluation results of ecosystem service value into ecosystem service management and land use planning and decision-making. For example, Li et al. (2018) found that the intervention of ecological restoration policy can improve the value of regional ecosystem services and promote the benign development of regional ecological environment (Li et al., 2018). Luo et al. (2020), by evaluating the ecosystem service value of China's Yangtze River Economic Belt, points out that the healthy development of the ecosystem in this region requires the protection and increase of the area of ecological land such as woodland and water area, to avoid the excessive transformation of ecological land into construction land (Luo et al., 2020). Thus it can be seen, quantitative assessment of ESV is clearly important for the effective conservation of ecosystems and the rational development of land resources.

Current assessments of ecosystem services mainly use monetary measurement, physical measurement, and energy analysis models (Zhan et al., 2019; Talukdar et al., 2020). Monetary assessment enables aggregation and comparison between different ecosystems. Monetary assessment results can be easily integrated into a national economic accounting system and are important for environmental accounting and the achievement of a "green" gross domestic product (GDP) (Fu, 2013). At the same time, monetization of ecosystem services can increase public awareness of the importance of ecosystem services for social development and help policymakers develop reasonable land-use plans (Su et al., 2020; Zhang et al., 2020b). The main methods of estimating ESV include the market price method, the productivity method, the travel cost method, and the benefit transfer method (King et al., 2000). Among these, the benefit transfer method is popular in decision-making when estimating ecosystem services at broad geographical scales because of its qualities of quick assessment and low cost of primary data collection (Song and Deng, 2017; Msofe et al., 2020; Liu et al., 2020). Costanza et al. (1997) first proposed this method in 1997 and evaluated the value of global ecosystem services. Based on the global equivalent factor table proposed by Costanza (1997), a large number of scholars have evaluated the value of ecosystem services in different countries and regions (Tory et al., 2006; Bateman et al., 2013; Kindu et al., 2016; Tolessa et al., 2017; Morshed et al., 2021). However, the evaluation of ecosystem service value through monetization is based on the determined value coefficient, which leads to some limitations of this assessment method. For one thing, the ascertainment of value coefficient is subjective to acertain extent (Wang et al., 2019; Xiao et al., 2020). For another, the value coefficient conforms to the reality of the study area directly affects the accuracy of the final ecosystem service value evaluation (Wu et al., 2020). Therefore, it is necessary to correct the value coefficient according to the actual situation of the study area (Wang et al., 2017; Rao et al., 2018; Xiao et al., 2020; Shi et al., 2021).

Ecosystem services exhibit complex interconnections and strong scale characteristics (MEA, 2005; Hu et al., 2015; Hou et al., 2020; Zheng et al., 2020). As the basis of all ecological studies, scale has always been the focus and difficulty of ecosystem services research (Sun et al., 2016, 2019; Pan and Li, 2017; Qiao et al., 2019; Bai et al., 2020; Zheng et al., 2020). Ecosystem processes and related ecosystem services are usually most significant and observable at a specific spatiotemporal scale, which can in some cases highlight dominant drivers or reveal a significant effect (MEA, 2005; Kindu et al., 2016). The complex characteristics of ecosystem services in response to changes in LULC derive primarily from spatial and temporal heterogeneities (Tolessa et al., 2017; Wang et al., 2017, 2018; Li et al., 2018). Temporal changes in ecosystems may have a limited impact on human well-being over the short term but can have significant long-term effects. An overly broad-scale spatial analysis can miss nuanced changes at a local level, whereas assessment results obtained using fine scales may be difficult to extrapolate to a large ecologically regulated region. Therefore, different spatiotemporal scales should be considered to investigate responses of ecosystem services to changes in LULC, and the selection of appropriate scales for assessment is essential for understanding the patterns and processes of regional ecosystems (Fu, 2013; MEA, 2005; Xiao et al., 2019). At present, most existing studies on the values and functions of ecosystem services focus on a single spatial scale, and no reasonable explanation has been given for the selection of research scale (Zhang et al., 2020b; Jiang et al., 2020; Msofe et al., 2020). In the time scale, the dynamic studies involving long time series are rare. Understanding the factors that lead to changes in ecosystems and their services is foundational for designing interventions to increase positive impacts and minimize negative impacts (MEA, 2005). Research conducted from different perspectives has shown that human activities are the main drivers of changes in ESV (Fang and Wang, 2013; Costanza et al., 2014; Tang, 2015; Xiao et al., 2019; Msofe et al., 2020). However, these drivers have mainly been identified using qualitative or semi-quantitative approaches (Hu et al., 2015; Li et al., 2018; Liu et al., 2020; Luo et al., 2020; Su et al., 2020). In addition, changes in ESV often result from interactions among multiple drivers (MEA, 2005; Gong et al., 2017; Luo et al., 2020). The synergistic roles of drivers should be considered to provide an accurate and comprehensive explanation of complex ESV changes.

As the most active ecosystem in the arid zone, changes in structure and function of the oasis region determine the stable and sustainable development of the regional social economy (Liu et al., 2010). Chinese oases are mainly distributed in the arid and semi-arid regions of northwest China and include Xinjiang, Gansu Hexi Corridor, and Ningxia-Inner Mongolia oases. The Hexi Corridor, located in key parts of the northwest regions of the ‘Silk Road Economic Belt’, is the main commodity grain base in northwest China and plays a special role in grain security (Guan et al., 2018).

The Shule River Basin is an ecological barrier for the Hexi Corridor and was a key construction area for testing ecological security defence systems in 2014. Since the 1980s, the Chinese government's ecological immigration policy has resulted in the movement of 143,900 people to the oases of the midstream and downstream reaches of the Shule River Basin (MDSB) (Chang and Zhang, 2014). The migration has increased the pressure on regional land resources and ecosystems and threatened regional ecological security (Ma et al., 2019). After 1997, Chinese government implemented a series of policies emphasizing regional development and environmental protection, such as "Reconstruction of Hexi Corridor", "Western Development", "Three-North Shelterbelt Project", "Grain for Green Project", etc., which directly or indirectly influenced land use in Shule River Basin (Ma et al., 2018). To test the effectiveness of ecological restoration policies and assess the impact of human activities on the ecosystem in different directions, it is necessary to study the changes of ecosystem service value in the study area in approximately the year 2000. Thus, the main objectives of this study are as follows: 1) to analyse the response of ESV to LULC changes in irrigated agricultural areas of the MDSB from 1977 to 2017; 2) to select an appropriate spatial scale for exploring spatial variation in ESV; and 3) to quantify the drivers of spatial differentiation of ESV. This study provides an important theoretical basis for the restoration of the ecological environment and the sustainable use of land resources in the study region and in other oases in arid and semi-arid regions worldwide.

2. Materials and methods

2.1 Study area

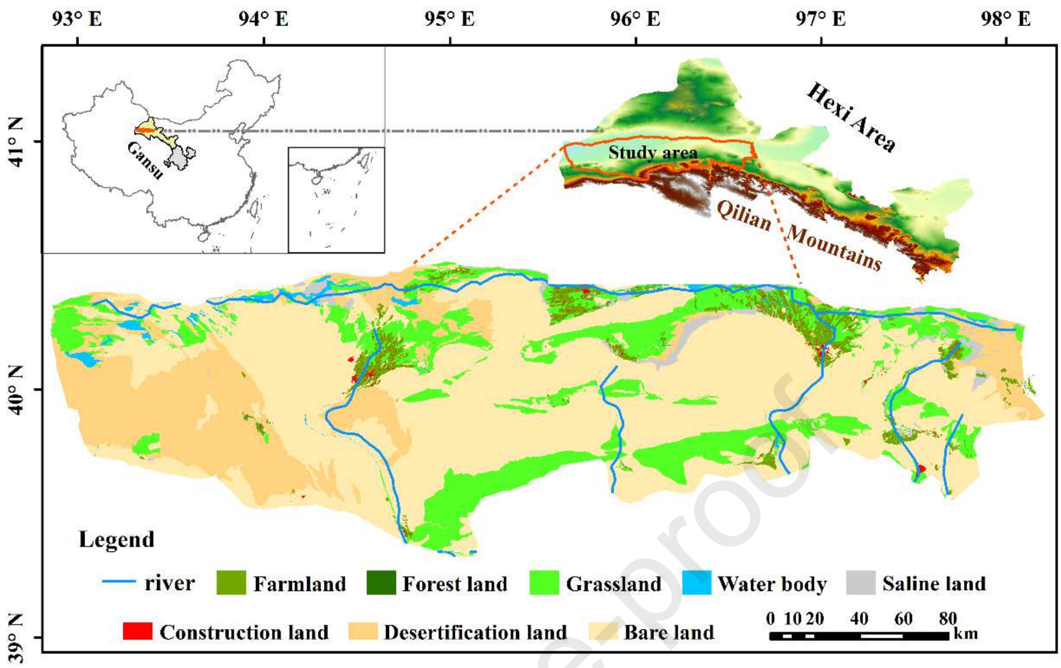

Fig. 1 Location of study area.

The Shule River originates from the western part of the Qilian Mountains (Fig. 1). With a main stem length of 630 km and a basin area of 38,147 km^2, the river has an average runoff of 1.07×10^9 m^3. The Shule River Basin is located mainly in the alluvial plain of the midstream and downstream reaches of the Shule River and in the sloping floodplain at the northern foot of the Qilian Mountains. It is an important part of the inland river basin in the Hexi region. In 2017, the total population was 504,000. The region clearly exhibits a temperate arid continental climate, with an average annual temperature of 7.04℃, annual average precipitation of 70.38 mm, and annual average evaporation of up to 3000 mm. The LULC is dominated by a desert landscape (Hao et al., 2018). Human activities in the basin are mainly concentrated in the oasis area of the plain in the midstream and downstream reaches. It is a typical irrigation area with the greatest area per capita of irrigated fields in the Hexi region and even in Gansu Province. The main crops are wheat and corn.

2.2 Data sources and processing

Considering the characteristics of image quality, cloud cover and vegetation growing season, the medium--resolution and high-resolution images of 20 scenes in 5 periods from 1977 to 2017 in the Shule River Basin were selected (Table S1). Meanwhile, the middle and lower reaches of Shule River are typical irrigated agricultural areas, the transformation of LULC by human activities is mainly for the purpose of developing agriculture. In addition, restricted by natural conditions (such as water resources), LULC changes slowly in the study area. Therefore, the change of LULC in the study area was analysed at an interval of ten years. ENVI 5.4 (EVIS Co., Colorado, USA), ERDAS 9.2 (ERDAS Co., California, USA), and ArcGIS 10.2 (ESRI, 2013) software are used to pre-process the image data to obtain the remote sensing image of the study area (Li et al., 2020, Fig. 2). Bands 7, 5, and 4 (R, G, and B, respectively) were used to interpret false-colour MSS composite images. Bands 4, 3, and 2 (R, G, and B, respectively) were used for the TM and OLI/TIRS images. To extract the actual surface status of the study region more accurately, the Land Use/Land Cover Remote Sensing Monitoring Data Classification System of the Resource and Environmental Science Data Centre of the Chinese Academy of Sciences (Xu et al., 2018) was referred to. A library of image interpretation signs of the study region was developed based on geographic knowledge and field research (Table S2). There were 8 types of LULC: farmland (FaL), grassland (GL), forest land (FoL), water body (WB), construction land (CL), desertified land (DL), saline land

191 (SaL), and bare land (BL). To facilitate the calculation of the service value of
192 different ecosystem types, the water body is divided into water area (WA) and
193 wetland (WL). The land-use classification system in this study consisted of different
194 levels of development of the same LULC types. Therefore, the grassland was
195 subdivided into high-coverage grassland (HG), moderate-coverage grassland (MG),
196 and low-coverage grassland (LG) and desertified land into severely desertified land
197 (SED), moderately desertified land (MD), slightly desertified land (SLD), and
198 potentially desertified land (PD).

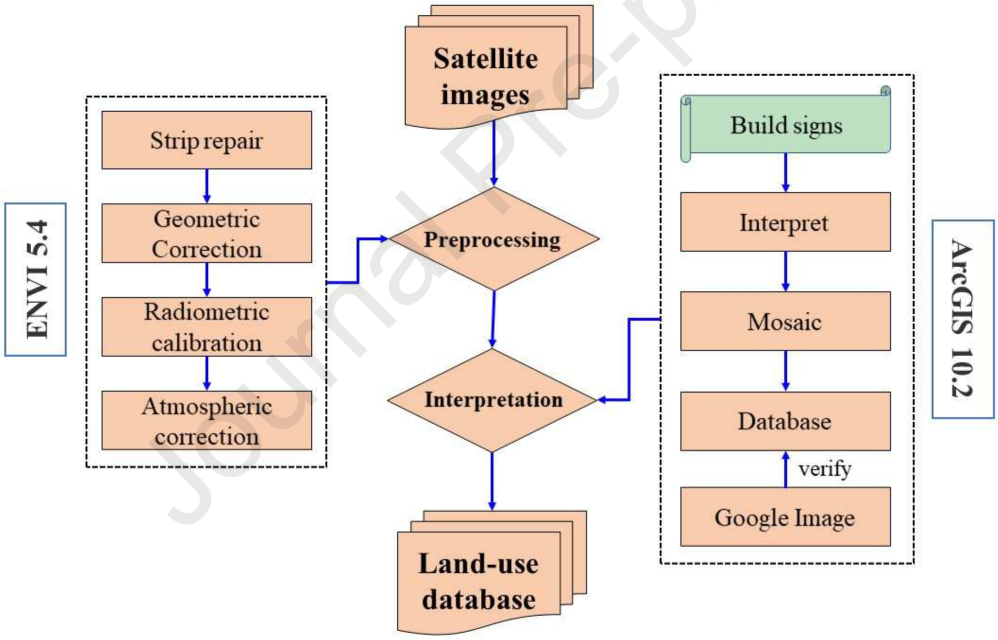

199 Fig. 2 The establishment process of land use database in the study area

200 To reduce the errors in visual interpretation, land-use information of the study
201 area in 2017 was extracted and corrected the results using high-resolution Google
202 Earth (Damtea et al., 2020) imagery and field observations to achieve accuracy
203 exceeding 85% (Wang et al., 2021). The images from the other 4 periods were then
204 corrected using the base map of the results of the interpreted data for 2017 that

passed the accuracy test. Thus, a land-use database was established for the MDSB from 1977 to 2017 (Table 3, Table S3; Fig. 4). The meteorological data and socioeconomic information used in this study are detailed in Table S3.

2.3 Methodology

2.3.1 LULC evolution analysis model

The parameters of single dynamic degree (K), comprehensive dynamic degree (K_S), and transfer matrix (K_{ij}) were used to describe the change in LULC in the study area (Redo et al., 2012).

1) Single dynamic degree (K) describes the change of a certain land use type in a certain period in the study area.

$$K = \frac{U_b - U_a}{U_a} \times \frac{1}{T} \times 100\% \tag{1}$$

where K refers to a single dynamic degree of LULC, U_a and U_b represent the areas of the specific LULC type at the start date and end date, respectively, and T indicates the monitoring period.

2) The comprehensive dynamic degree (K_S) was used to characterize the rate of land use change in the whole study area.

$$K_s = \sum_{i=1}^{n} \left| u_{bi} - u_{ai} \right| / 2 \sum_{i=1}^{n} u_{ai} \times \frac{1}{T} \times 100\% \tag{2}$$

where Ks refers to the comprehensive dynamic degree of LULC, u_{ai} and u_{bi} represent the areas of the specific LULC type at the start date and end date, respectively, T indicates the monitoring period, and n is the number of the LULC type.

3) The land use transfer matrix (K_{ij}) is used to represent the dynamic transformation of each land use type in the research period.

$$K_{ij} = \begin{vmatrix} K_{11} & K_{12} & \ldots & K_{1n} \\ K_{21} & K_{22} & \ldots & K_{2n} \\ \ldots & \ldots & \ldots & \ldots \\ K_{n1} & K_{n2} & \ldots & K_{nn} \end{vmatrix} \quad (3)$$

where K is the LULC area, n is the number of LULC types, and i and j are the LULC types at the start and at the end, respectively.

2.3.2 Estimation of ESV

In 1997, Costanza et al. (1997) proposed a global scale ecosystem services value evaluation method system and evaluated the economic value of 17 ecosystem services in 16 biomes around the world. However, because this system is not fully applicable to China's ecological background, Chinese scholar Xie et al. (2008) referred to the method of Costanza et al. (1997) and conducted a questionnaire survey of 500 Chinese ecologists, and summarized an equivalent factor of ESV per unit area suitable for an evaluation of ecosystem service value at the Chinese scale. This paper uses the framework of Costanza et al. (1997), but employed ESVs developed for China by Xie et al. (2008), which is based on the data in MEA (2003, 2005) and the understanding of ecosystem services provided by Chinese researchers, the 17 ecosystem services proposed by Costanza et al. (1997) are divided into four types and nine sub-types: provision services (include Food production-FP and Raw material production-RMP), Regulation service (include Gas regulation-GR, Climate regulation-CR, Hydrological regulation-HR and Waste decomposition-WD), Support services (include Soil conservation-SC and Biodiversity protection-BP) and Cultural services (Provide aesthetic landscape-PAL) (Table 1).

Ecosystem service value equivalent factor refers to the potential capacity of the relative contribution of ecological services generated by the ecosystem, which is defined as the economic value of the annual natural grain production of farmland with the national average yield of 1hm^2. Based on this, the weighting factor table can be converted into the unit price table of ecosystem services in the current year. After comprehensive comparative analysis, the economic value of the equivalent factor of ecosystem service value is determined to be 1/7 of the regional average market value of grain yield per unit area (Xie et al., 2003). Based on this, the ecosystem service equivalent factor in the study area is modified, and the formula is as follows:

$$Ea = \frac{1}{7} \times \sum_{i=1}^{n} \frac{m_i p_i q_i}{M} (i = 1, \ldots n) \tag{4}$$

where Ea represents the economic value of food production service provided per unit area of farmland (Yuan/hm^2), i is the crop species, p_i is the average crop price (Yuan/t), q_i refers to the yield of crop per unit area of i (t/hm^2), m_i refers to area of i (hm^2), and M refers to the total area of grain crops (hm^2). In this study area, Ea is 1957.75 Yuan/hm^2.

The ESV per unit area of an ecosystem (VC) is calculated using Eq. (5):

$$VC = E\mathrm{a} \times Q \tag{5}$$

where Q refers to the ESV equivalent coefficient per unit area proposed by Xie et al. (2001, 2015). The ESV equivalents per unit area of different LULC types in the MDSB were then determined (Table 1).

Table 1 ESV per unit area of different LULC types in the MDSB (Yuan/hm^2) (2015 prices)

Service type categories	Service type subcategories	FoL	GL	FaL	WL	WA	UL	Total
Provision services	FP	646.06	1367.68	1957.75	704.79	1037.61	39.16	5753.05
	RMP	5834.11	21.71	763.52	469.86	685.21	78.31	7852.73
Regulatory services	GR	8457.50	162.82	1409.58	4718.19	998.45	117.47	15864.01
	CR	7968.06	893.70	1899.02	26527.57	4032.97	254.51	41575.82
	HR	8007.21	806.86	1507.47	26312.21	36747.04	137.04	73517.84
	WD	3367.34	2532.74	2721.28	28191.66	29072.65	509.02	66394.68
Support services	SC	7870.17	589.77	2877.90	3895.93	802.68	332.82	16369.26
	BP	8829.47	1005.86	1996.91	7224.11	6715.10	783.10	26554.55
Cultural services	PAL	4072.13	325.64	332.82	9181.87	8692.43	469.86	23074.74
	Total	55052.04	7706.78	15466.3	107226.2	88784.14	2721.3	276956.68

Notes: Provision services--Food production (FP) and Raw material production (RMP); Regulatory services--Gas regulation (GR), Climate regulation (CR), Hydrological regulation (HR), and Waste decomposition (WD); Support services--Soil conservation (SC) and Biodiversity protection (BP); and Cultural services (Provide aesthetic landscape--PAL).

The formula for calculating total ESV is:

$$ESV = \sum_{i=1}^{m} \sum_{k}^{n} A_{ik} \times VC_{ik} \tag{6}$$

where A_{ik} is the area (hm^2) of the i-th LULC type, VC_{ik} represent the value coefficient of the i-th LULC type corresponding to the k-th service (Table 1), i is the number of LULC types, k is ecosystem service types, m = 6, and n = 9.

2.3.3 ESV sensitivity analysis

Considering uncertainties of the value coefficients (VC), the value coefficients for each LULC category were adjusted by 50%, and the estimated ESV results were verified by the coefficient of sensitivity index (Kreuter, 2001). The formula is:

$$CS = \left| \frac{(ESV_j - ESV_i) / ESV_i}{(VC_{\mathrm{jk}} - VC_{\mathrm{ik}}) / VC_{\mathrm{ik}}} \right| \tag{7}$$

where ESV_i and ESV_j represent initial and adjusted total estimated ESV, respectively, and VC_{ik} and VC_{jk} are initial and adjusted *VC* for LULC category *k*. *CS* is an important index for measuring the extent of ESV change caused by 1% change in *VC*. If $CS > 1$ (< 1), for every 1% increase or decrease in *VC*, the increase or decrease in *ESV* is greater (less) than 1%, indicating the *ESV* is high (low) in elasticity relative to *VC* and reflecting low (high) credibility of evaluation results. The greater the proportional change in *ESV* relative to the proportional change in *VC*, the more critical is the use of an accurate ecosystem *VC* (Liu et al., 2012).

2.3.4 Spatial heterogeneity analysis of ESV

Exploratory spatial data analysis (ESDA) involves the use of spatial analysis techniques to visualize the spatial distribution patterns of objects or phenomena (Good, 1983; Symanzik et al., 2013). This paper makes use of GeoDa statistical software (Anselin et al., 2002), ESDA method was used to investigate the impact of four types of scale (2 km × 2 km, the township administrative unit, the watershed unit, and the county administrative unit) changes on ESV in the middle and lower reaches of the Shule River. Based on the results, appropriate research scales were selected to analyse spatial heterogeneity in ESV.

In this study, the global spatial autocorrelation Moran's *I* from the ESDA analysis method was selected to reflect the spatial heterogeneity of ESV, and it can be calculated as follows (Moran, 1950).

$$Moran's\ I = \frac{n\sum_{i=1}^{n}\sum_{j=1}^{n} W_{ij}(x_i-\bar{x})(x_j-\bar{x})}{\sum_{i=1}^{n}\sum_{j=1}^{n} W_{ij}\sum_{i=1}^{n}(x_i-\bar{x})^2} \tag{8}$$

where n is total number of ESV evaluation units; x_i (x_j) is the observation value of ESV evaluation units i (j); W_{ij} is spatial weight between ESV evaluation units i and j; and $\overline{x}$ is the mean value of ESV evaluation units. The range of the Moran's I value is [-1, 1]. When the value of Moran's I approaches 1, there is a clustered pattern for the indicator. When the value of Moran's I is close to -1, there is a dispersed pattern for the indicator. When the value of Moran's I is equal to 0, it indicates that ESV values are randomly distributed in the region and have no spatial autocorrelation.

The final conclusions about the observed pattern are drawn only after looking at the Z-score and the p-value of the Index. To investigate the statistical significance of the Moran's I statistic, $Z(I)$ is calculated as follows:

$$Z(I)=\frac{1-E(I)}{\sqrt{\mathrm{Var}(I)}} \tag{9}$$

where $E(I)$ is the expected value of I: $E(I) = -1/(n-1)$, and $\sqrt{\mathrm{Var}(I)}$ is the expected variance of I: $\sqrt{\mathrm{Var}(I)} = E(I^2)-E(I)^2$. When the P-value obtained is greater than 0.05, the basic assumption is accepted implying that the data values are randomly spread out spatially. When the p-value is less than 0.05 and the Z-score is negative, the basic assumption of randomness is rejected, inferring that the high and the low values in the dataset are dispersed spatially. Similarly, when the p-value is less than 0.05 with a positive Z-score, the assumption of randomness is again ruled out and the inference drawn is that the high and/or low data values are spatially clustered in the geographical space (Yang et al., 2018; Kumari., 2019).

2.3.5 Driving force of spatial heterogeneity analysis of ESV

Temporal and spatial variation in ESV is the result of many synthetic factors (Chen et al., 2020). Based on the spatial variation theory, Geographical Detector model (GDM) is designed to measure spatially stratified heterogeneity of a response variable and reveal the impact of driving factors (Wang et al., 2010). The hypothesis of GDM is that if an environmental factor (*X*) contributes to a response variable (*Y*), there may be a similar spatial distribution for the two, and this similarity or spatial association can be measured by the *q*-statistics (Fig. 3, Wang et al., 2016). By superposing the independent variable spatial distribution layer and the dependent variable spatial distribution layer, the variance σ_i^2 of ESV in each sub-region and σ^2 in the whole region are calculated. The value of *q* indicates that the independent variable *X* explains 100×*q*% of the dependent variable *Y*. The larger the *q* value, the stronger the explanatory power of the independent variable *X* to the dependent variable *Y*, and the weaker the opposite. GDM includes a differentiation and factor detector, an interaction detector, an ecological detector, and a risk detector. According to the research objectives of this paper, differentiation and factor detectors (compares the accumulated dispersion variance of each subregion with the dispersion variance of the entire study region; the smaller the ratio, the stronger the factor contribution of the stratum) and interaction detectors (compares the sum of the contribution of two individual attributes versus the contribution of the two attributes when taken together) were selected.

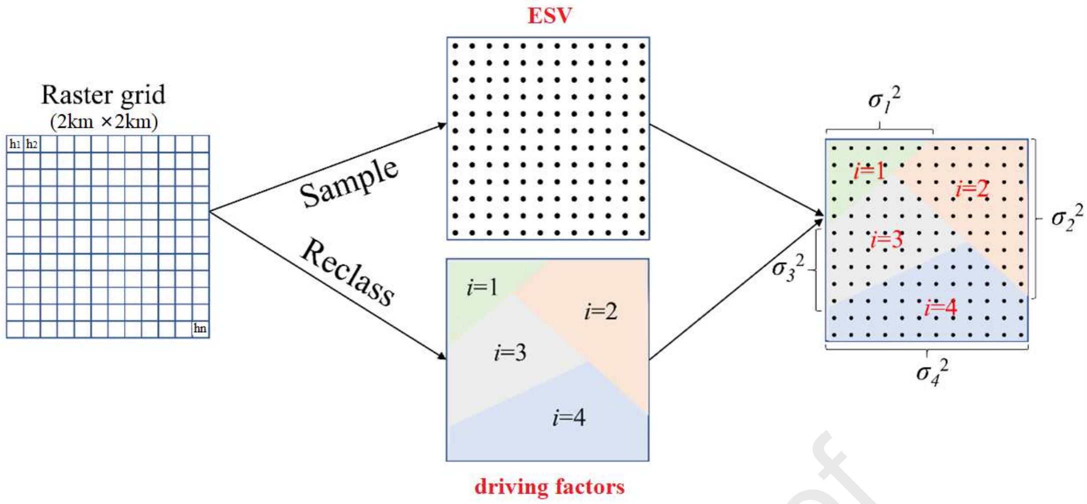

Fig. 3 The principle of geographical detector models

A differentiation and factor detector can be used to detect spatial differentiation of ESV and the extent to which factor *X* explains the spatial variation in ESV. Measured with the *q* value, the expression is as follows:

$$q = 1 - \frac{\sum_{h=1}^{L} N_h \sigma_h^2}{N\sigma^2} \tag{10}$$

where *h* = 1, 2,..., *L* is the stratification of ESV or factor *X*, *N* is the number of samples, σ^2 represents the variance in ESV, and *q* signifies the degree of explanation of ESV by factor *X*. The value range of *q* is 0 to 1. When the value of *q* = 1, factor *X* completely controls the spatial distribution of ESV; *q* = 0 indicates that there is no association between *X* and ESV.

The interaction detector is defined to identify the interaction between different factors by comparing *q* ($X_1 \cap X_2$) with *q* (X_1) and *q* (X_2). The possibilities for interaction between the factors include nonlinear weakening, nonlinear weakening of one factor, bilateral enhancement of both factors, both factors acting independently, and nonlinear enhancement. Detailed principles can be found in published literature

(Wang et al., 2016).

Table 2 Data sources and processing

	Driving factors	Sources	Processing
Nature factors	Temperature (Tem)	http://data.cma.cn/	Anusplin interpolation model
	Precipitation (Pre)		
	Elevation		
	Slope		
	Net Primary Productivity (NPP)	https://data.tpdc.ac.cn	ArcGIS Spatial analysis function
	Normalized Difference Vegetation Index (NDVI)		
Human factors	Gross Domestic Product (GDP)	http://www.resdc.cn/	
	Population (POP)		
	Road density	http://www.webmap.cn/	
	Human activity intensity (HAI)	Xu et al., 2016	$HAI = \frac{Acle}{A} \times 100\%$ $Acle = \sum_{i=1}^{m} (ALi \bullet CIi)$
	Land use intensity (LA)	Zhuang and Liu, 1997	$La = 100 \times \sum_{i=1}^{n} Ai \times Ci$
Landscape pattern factors	Landscape Division Index (DIVISION)	LULC data	Fragstats software 4.2
	Shannon's Diversity Index (SDI)		
	Mean Shape Index (MSI)		
Statistic data	total population	National/Local Bureau of Statistics	
	the total production value of three industries		
	rural per capita net income		

Fourteen factors were selected from three categories to study the spatial differentiation mechanism of ESV in the entire MDSB: natural factors (elevation, slope, temperature (Tem), precipitation (Pre), NPP, and normalized difference vegetation index (NDVI)), human factors (average GDP, population density, human activity index (HAI), land-use intensity (LA), and road density), and landscape factors (the Shannon diversity index (SDI), the mean shape index (MSI), and the landscape division index (DIVISION)) (Table 2). Then the degree of correlation between each factor and ESV differentiation was calculated.

3 Results

3.1 LULC dynamics

Table 3 Area and dynamic degrees (*K*) of various LULC types in the MDSB from 1977 to 2017

LULC type	Area (km^2)					K (%)				
	1977	1987	1997	2007	2017	1977-1987	1987-1997	1997-2007	2007-2017	1977-2017
FaL	1323.3	1340.5	1416.2	1781.3	1949.1	0.13	0.56	2.58	0.94	1.18
GL	6787.4	6782	6829.4	6417.6	6556.4	-0.01	0.07	-0.60	0.22	-0.09
FoL	11	10.2	8.1	6.9	7.4	-0.68	-2.05	-1.50	0.74	-0.81
SaL	753.5	758.4	754	592.3	511	0.07	-0.06	-2.14	-1.37	-0.80
CL	109.4	122.5	137.2	134.4	167.1	1.20	1.20	-0.21	2.44	1.32
WB	358.9	362.2	366.8	331.9	409.2	0.09	0.12	-0.95	2.33	0.35
DL	7033.5	7044.4	7052.2	6607.2	6584.8	0.02	0.01	-0.63	-0.03	-0.16
BL	21769.7	21727	21582.8	22275	21961.9	-0.02	-0.07	0.32	-0.14	0.02

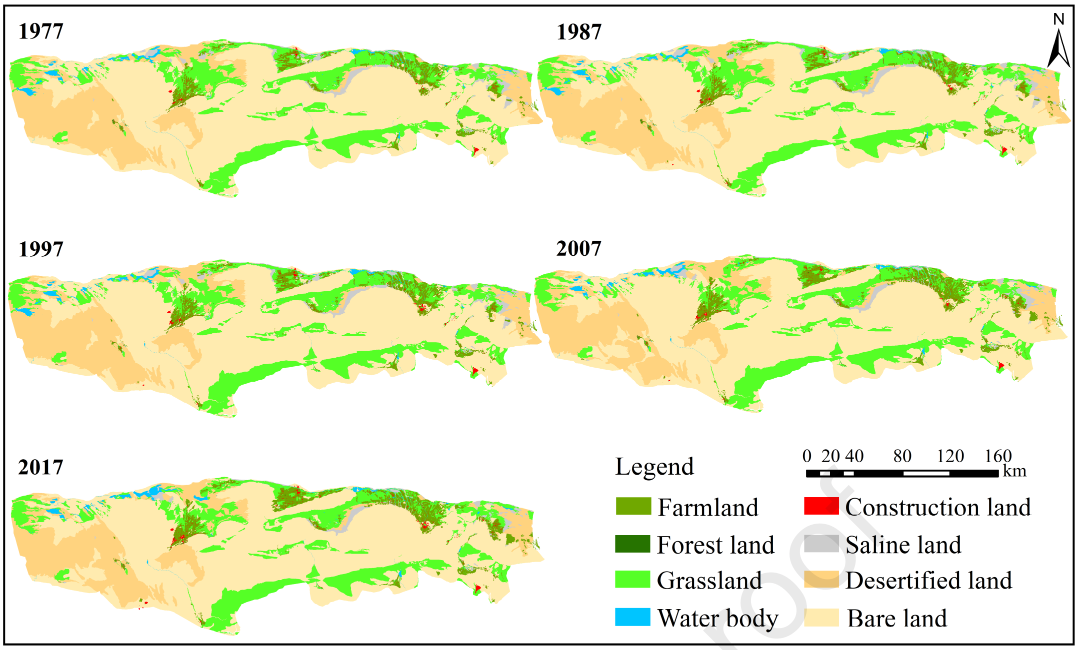

Fig. 4 LULC maps of study area from 1977-2017.

Change in LULC in the study region was concentrated in the oases and peripheral areas with intensive human activities. Changes were particularly observable in farmland, construction lands, and high-coverage grassland (Table 3, S3, Fig. 4). Farmland continued to expand during the 41-year study period, with an increase in area of 625.8 km^2 at an expansion rate reaching 15.3 km^2/a and a dynamic degree of 1.18%. It was mainly transferred from grassland, desertified land, and saline land (Fig. 5). Construction lands were scattered around farmland and underwent significant growth during the study period. The growth rate reached 52.72%, where the greatest contribution to the total increase in construction land occurred from 2007 to 2017. Bare land and grassland were the main components of the study region. Bare land was the dominant component and remained largely stable over the study period (with a dynamic degree approximately 0). Water bodies showed a slow increase with fluctuations over the 41 years, with a total expansion of 50.3

km^2. The most rapid expansion for water bodies occurred from 2007 to 2017, with a dynamic degree of 2.33% (Table 3, Fig. 4).

In addition, it should be noted that although the overall grassland showed a slight trend of shrinking, the growth rate of high-cover grassland was much higher than that of low-cover grassland and medium-cover grassland. The desertified land showed negative growth overall, and the severely desertified land reversed obviously (Table S3). The LULC conversion dynamics showed the conversion of grassland and desertified land occurred mainly between different levels of the same category, both with positive trends. For example, the main contributions to moderate-coverage grassland and high-coverage grassland were low-coverage grassland (62.51%) and moderate-coverage grassland (90.64%); Severely and moderately desertified land constituted the main contributing sources to slightly desertified land. It shows that the land cover environment in the study area is relatively improved.

In general, the change in LULC was complex during the 41 years in the MDSB, with changes in land cover mainly occurring with concentrated human activities. The fluctuations in LULC were small throughout the study period, with a K_s of only 0.092%. However, the Ks from 1997 to 2007 was as high as 0.359%. The LULC conversion dynamics showed an overall improvement in the ecological environment of the study area during the investigated period.

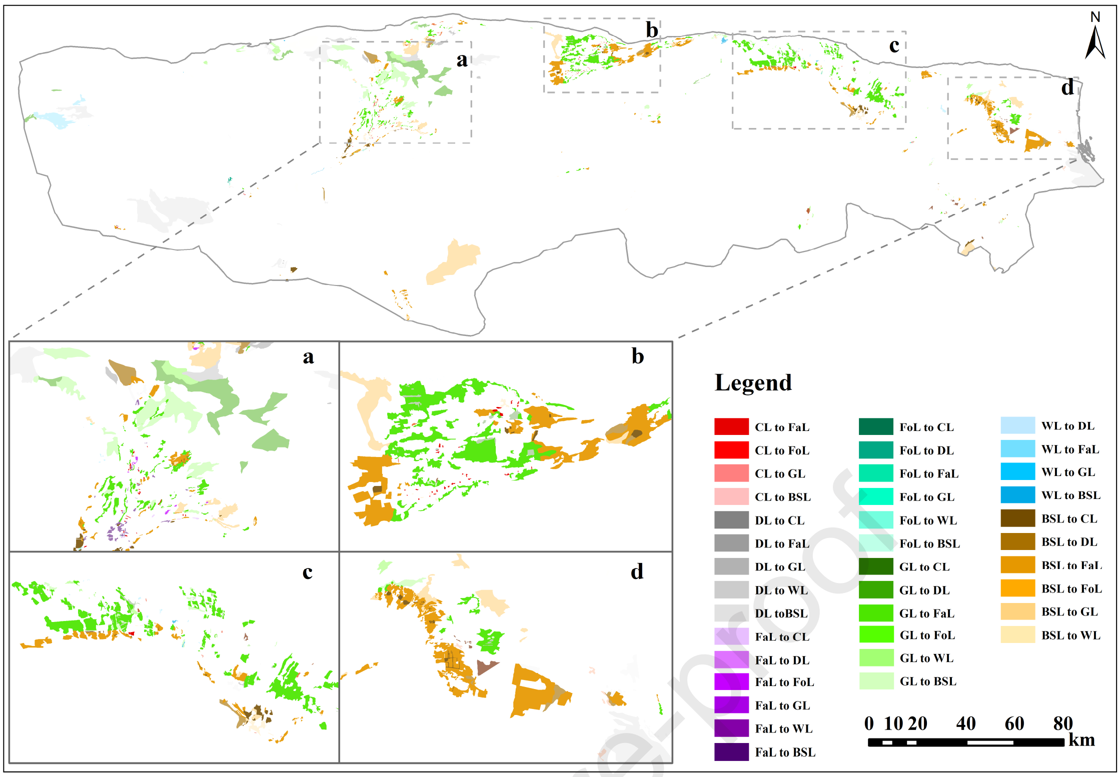

Note: BSL refers to bare and saline land.

Fig. 5 Spatial distribution of LULC in the study area from 1977 to 2017.

3.2 Estimation of changes in ESV

Based on the value per unit area of ecosystem services for each LULC type in the study region and the LULC database (Table 1, 3), the ESV and ESV_f in the MDSB were estimated. The results showed an increasing overall trend in ESV in the study region from 1977 to 2017, with a total increment of 1.01×10^9 Yuan and an average annual growth rate of 113% (Table 4). Unused land, which accounted for approximately 78% of the study region, contributed the most to ESV (39.45 - 42.42%), followed by grassland (25.21 - 27.48%). Although the former exhibited the greatest contribution rate, the contribution to ESV (approximately 60%) from other LULC types, comprising approximately 22% of the study region, was more concerning (Tables 3, 4). In terms of the increasing trend in ESV, farmland was the main contributor (95.9%), followed by water bodies (78.5%). Except for the time from 1997 to 2007, the ESV in the study area displayed a growth trend. The LULC type contributing the most to ESV growth from 1987-1997 was farmland (81% contribution). 1977-1987 and 2007-2017, wetland contributed the most (contributions of 101% and 144%, respectively; Table 4).

Table 4 Change in ESV in study area from 1977 to 2017 ($\times 10^6$ yuan)

	Year	FoL	GL	FaL	WL	WA	UL	Total
Ecosystem services value	1977	60.34	5230.91	2046.71	2722.17	932.06	8043.18	19035.36
	1987	56.21	5226.74	2073.24	2800.43	897.34	8035.88	19089.83
	1997	44.70	5263.23	2190.35	2803.96	934.54	7997.53	19234.32
	2007	37.99	4945.87	2755.05	1158.04	1988.14	8020.82	18905.92
	2017	40.79	5052.87	3014.56	2304.29	1724.99	7907.41	20044.91
Change (%)	1977-2007	-37	-5	+35	-57	+113	0.00	-1
	2007-2017	+7	+2	+9	+99	-13	-1	+6
	1977-2017	-32	-3	+47	-15	+85	-2	+5

Notes: “+” means increase and “-” means decrease.

Table 5 The values of individual ecosystem functions (ESV_f) in the study area from 1977 to 2017 ($\times 10^6$ yuan)

		1977		1987		1997		2007		2017	
Service type categories	Service type subcategories		%		%		%		%		%
Provision services	FP	1332.60	7.00	1335.17	6.99	1356.25	7.05	1370.08	7.35	1427.86	7.12
	RMP	372.75	1.96	373.47	1.96	377.34	1.96	403.17	2.16	418.34	2.09
Regulatory services	GR	783.77	4.12	788.20	4.13	796.80	4.14	778.00	4.17	849.88	4.24
	CR	2334.66	12.26	2353.94	12.33	2369.87	12.32	2032.31	10.90	2349.96	11.72
	HR	2214.73	11.63	2220.75	11.63	2248.64	11.69	2193.92	11.77	2506.39	12.50
	WD	4608.27	24.21	4619.16	24.20	4656.99	24.21	4482.10	24.04	4843.25	24.16
Support services	SC	1880.80	9.88	1886.46	9.88	1905.18	9.91	1935.20	10.38	2019.86	10.0
	BP	3525.13	18.52	3527.90	18.48	3537.95	18.39	3523.96	18.90	3616.47	18.04
Cultural services	PAL	1982.63	10.42	1984.77	10.40	1985.30	10.32	1924.02	10.32	2012.90	10.04
	Total	19035.4	100	19089.8	100	19234.3	100	18642.8	100	20044.9	100

Definitions of acronyms given in Table 1, and % represents the percentage of ESV_f in the total ESV.

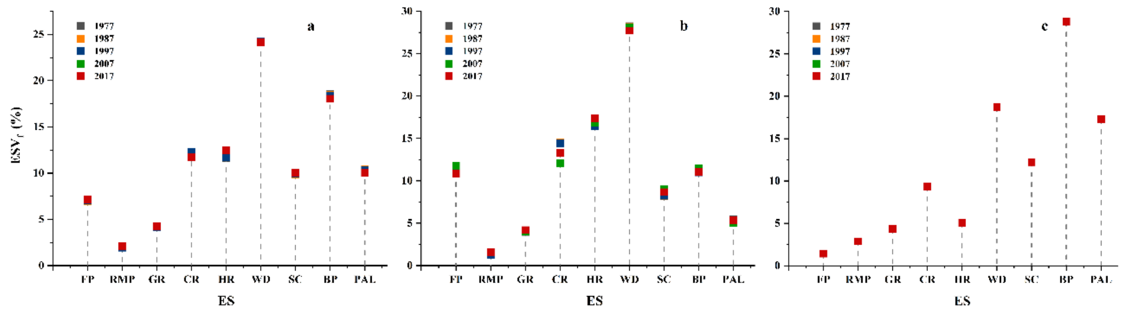

Definitions of acronyms given in Table 1.

Fig. 6 Dynamics of ESV_f for study area (a), oasis system (b) and desert system (c) from 1977 to 2017. Definitions of acronyms given in Table 1.

The values of individual ecosystem functions (ESV_f) in the study region generally showed increasing trends, but variation among these functions was evident (Fig. 6a). Among all services, waste disposal (24%) and biodiversity conservation (18%) made up the greatest portions of the total ESV. The phase analysis showed that the increases in total ESV from 1977 to 1997 and from 2007 to 2017 and the decrease from 1997 to 2007 were mainly caused by increases and decreases, respectively, in the value of regulatory services (including waste decomposition, climate regulation, and hydrological regulation; Table 5, Fig. 6a). The most severely impacted regulatory service from 1997 to 2007 was the climate regulating service, the value of which decreased by 14.24% over the 11 years (Table 5, Fig. 6a). In addition, an analysis of ESV_f in oasis and desert ecosystems found that the increases and decreases in ESV_f throughout the study region were largely dominated by the oasis ecosystems. The value of the waste disposal service made up the largest proportion (Figs. 6a, 6b). ESV_f of desert ecosystems remained largely stable throughout the 41 years, and biodiversity conservation was strongest among all services (Fig. 6c).

The *CS* values of different periods and different LULC types were all less than 1 and changed little in each period (Table 6). These results confirmed that the total ESV estimated in this study area was inelastic relatively to the *VC*. In addition, these findings indicate that the change in the corresponding *VC* has a relatively small impact on ESV in the study area. The adjusted equivalent factor can reasonably evaluate the fluctuation of ESV in the MDSB. The *CS* values of unused land and grassland were higher than those for other LULC types, indicating that these 2 land types greatly impacted ESV (Table 6).

Table 6 The results of a sensitivity test (*CS*) for ESV in the MDSB

Time	FoL	GL	FaL	WL	WA	UL
1977	0.010	0.550	0.215	0.286	0.098	0.845
1987	0.009	0.548	0.217	0.293	0.094	0.842
1997	0.007	0.547	0.228	0.292	0.097	0.823
2007	0.006	0.523	0.291	0.123	0.210	0.848
2017	0.010	0.504	0.301	0.230	0.172	0.789

3.3 Spatial heterogeneity of ESV

The selection of an appropriate scale for the assessment unit can elucidate spatial differentiation in the ESV over the study region. An analysis of the spatial distribution of ESV at different scales showed that the smaller the assessment unit was, the finer the resulting ESV spatial distribution was. ESV spatial distributions at the watershed, township, and county scales varied significantly from that at the grid scale (Fig. 7). The use of a large assessment unit filtered out originally existing differentiated information, resulting in less precise assessment results. Results of the analysis showed that the changes in ESV occurred mainly within the oases (which comprised only approximately 22% of the total area) and were directly caused by conversions and changes in LULC (Table 4, Fig. 6). Therefore, the ESV assessment unit needs to reflect small-scale information about the oasis zone. Results of global spatial autocorrelation analysis showed that Moran's *I* values for ESV at the grid, watershed, township, and county scales were 0.672, 0.010, 0.055, and -0.249, respectively. The *P*-value for the grid scale was less than 0.001. The other 3 scales did not pass the significance test, showing that the grid scale best represented the spatial differentiation characteristics of the regional ESV. Therefore, the assessment unit scale of 2 km × 2 km was selected to analyse the spatial distribution characteristics of ESV for the study region.

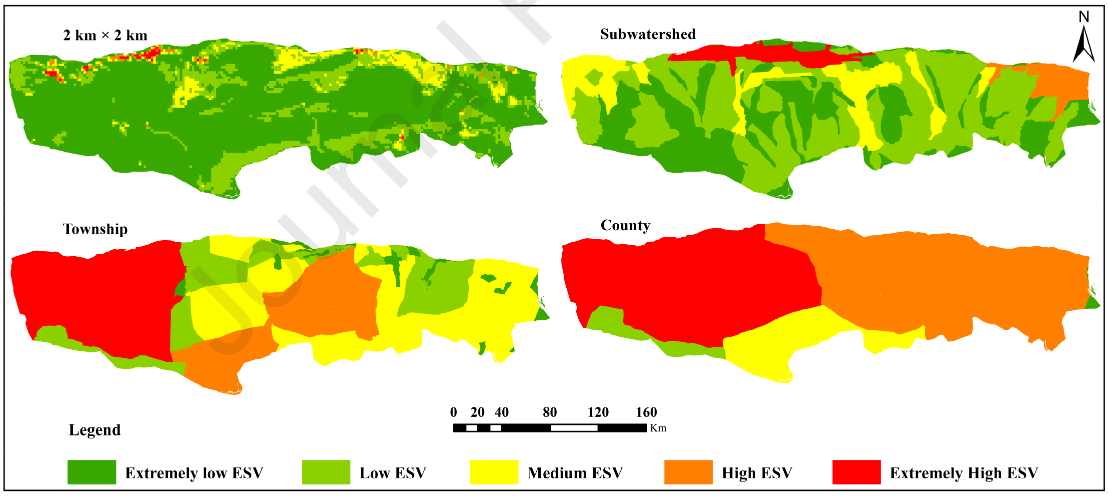

Fig. 7 Spatial distribution characteristics of ESV in study area under different spatial scales.

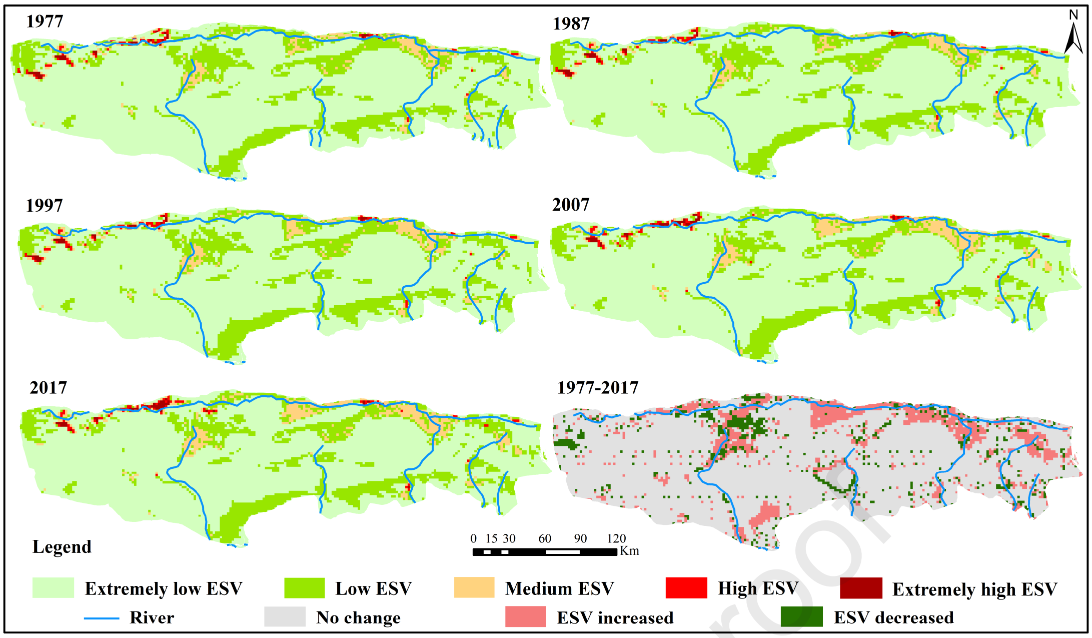

Fig. 8 Spatial distribution of ESV in the MDSB.

The ESV results for the study region were divided into 5 levels using natural breaks classification in ArcGIS 10 software (Fig. 8). The spatial distribution in ESV did not change significantly over the 41 years. Extremely high ESV (27.42-42.89, $\times 10^6$ Yuan) and high ESV (12.59-27.42, $\times 10^6$ Yuan) were found for points and patches scattered over water-rich regions along the main flow of the northern Shule River. Medium-ESV (4.68-12.59, $\times 10^6$ Yuan) regions mainly consisted of farmland and continued to expand. Regions with extremely low ESV (0-2.09, $\times 10^6$ Yuan) and low ESV (2.09-4.68, $\times 10^6$ Yuan) were continuous areas of mainly unused land (Figs. 4, 8). The portions of the study region for which ESV increased were mostly contiguous areas distributed over agricultural areas with adequate water supplies. The principal constituent LULC types were farmland and water bodies. Decreases in ESV mostly occurred at scattered points and in patches, mainly because of grassland shrinkage (Figs. 4, 8). A global autocorrelation analysis of ESV from 1977 to 2017 at the 2 km × 2 km scale resulted in a Moran's *I* above 0 for all 5 periods at the 0.1% significance level, indicating strong positive spatial correlation in ESV. Moran's *I* dropped to its lowest value in 2007 but increased both before and after 2007. Most grid cells were within high-high or low-low aggregation areas. Aggregations with high and low ESV were observed (Table 7, Fig. 8).

Table 7 Global Moran's *I* of ESV in the MDSB, 1977-2017

Year	1977	1987	1997	2007	2017
Moran's *I*	0.637	0.641	0.642	0.627	0.672
Z (*I*)	86.519	87.035	87.004	89.401	97.246
P-value	0.001	0.001	0.001	0.001	0.001

3.4 Driving force of spatial heterogeneity in ESV

Table 8 The contributions (*q* statistics) of different factors to ESV variation

	Variables	*q*-Statistic	P-value
X_1	Tem	0.031	0.000
X_2	Pre	0.020	0.000
X_3	Elevation	0.067	0.000
X_4	Slope	0.012	0.000
X_5	NPP	0.019	0.000
X_6	NDVI	0.050	0.000
X_7	GDP	0.030	0.000
X_8	POP	0.030	0.000
X_9	Road density	0.003	0.008
X_{10}	HAI	0.115	0.000
X_{11}	LA	0.147	0.000
X_{12}	DIVISION	0.086	0.000
X_{13}	SHI	0.110	0.000
X_{14}	MSI	0.036	0.000

The differentiation and factor detection results showed that all the variables passed the 0.5% significance test, except for the road density. Thus, multiple factors influenced the spatial differentiation of ESV for the study region (Table 8). The *q* values were ranked as follows: LA (0.147) >HAI (0.115) > SDI (0.110) > DIVISION (0.086) > elevation (0.067) > NDVI (0.050) > other factors (< 0.036). LA was the dominant factor influencing the spatial differentiation of ESV in the study region. Human factors and landscape factors influenced ESV more significantly than did natural factors.

Table 9 Interactive effects between the factors

	Tem	Pre	Elevation	Slope	NPP	NDVI	GDP	POP	R-density	HAI	LA	DIVISION	SDI	MSI
Tem	0.031													
Pre	0.046	0.020												
Elevation	0.069	0.077	0.067											
Slope	0.040	0.033	0.075	0.012										
NPP	0.052	0.040	0.089	0.030	0.019									
NDVI	0.120	0.113	0.167	0.072	0.059	0.050								
GDP	0.065	0.059	0.111	0.039	0.038	0.068	0.030							
POP	0.062	0.053	0.111	0.039	0.040	0.069	0.043	0.030						
R-density	0.036	0.027	0.073	0.016	0.022	0.053	0.033	0.033	0.003					
HAI	0.204	0.216	0.250	0.143	0.118	0.136	0.124	0.124	0.117	0.115				
LA	0.240	0.249	0.284	0.187	0.147	0.160	0.153	0.153	0.148	0.178	0.147			
DIVISION	0.126	0.121	0.151	0.096	0.096	0.109	0.102	0.102	0.090	0.174	0.199	0.086		
SDI	0.151	0.151	0.183	0.120	0.120	0.130	0.134	0.134	0.112	0.185	**0.205**	0.119	0.110	
MSI	0.077	0.068	0.100	0.049	0.052	0.076	0.055	0.055	0.040	0.143	0.165	0.097	0.121	0.036

Note: Yellow represents bilateral enhancement of both factors, and grey represents nonlinear enhancement.

The interaction detection results showed that the interactions between pairs of the selected factors exhibited more highly significant effects than did any single factor, and the interaction type was mainly manifested as bilateral enhancement of both factors (Table 9). LA and HAI exerted strong influences on the factor interactions, and the q values of the interactions of other factors with LA and HAI were several times higher than values for the independent actions of these factors. The interactions of LA and HAI with natural factors (elevation, Pre, and Tem) exhibited the most significant effects on ESV, with average q values exceeding 0.2. LA ∩ elevation featured the highest q value of 0.284 and the greatest impact on spatial differentiation of ESV over the study region. The q values of LA and the landscape factor SDI also exceeded 0.2. Consequently, the spatial differentiation of ESV in the MDSB resulted from a combination of human factors, natural factors, and landscape factors, of which human factors exerted the most significant influence.

4 Discussion

4.1 Changes in ESV and LULC change

The study results showed small overall changes in the LULC of the study region, indicating an extremely stable ecosystem structure in the area (Table 3, Fig. 4). Complex dynamic conversions between different land-use categories and different levels within a category occurred during the study period. The conversions mainly occurred in irrigation districts in oases, where human activities were concentrated (Table 3, S3, Fig. 4). This result corresponds to one of the main characteristics of resource use in arid regions in China (Abulizi et al., 2017; He et al., 2017; Wang et al., 2017; Wei et al., 2018; Yushanjiang et al., 2018; Zhang et al., 2020b). Significant expansion of farmland and construction lands occurred as a result of unidirectional conversions from other LULC types. This pattern has also been found in other studies of oases in arid regions (Lü et al., 2014; Abulizi et al., 2017; Tolessa et al., 2017; Wang et al., 2017; Wei et al., 2017; Rukundo et al., 2018; Wei et al., 2018; Yushanjiang et al., 2018; Wang et al., 2020). The source LULC types that were converted to farmland were largely low-coverage grassland and saline land, which had unstable ecosystems (Fig. 4, Table S4). This result shows that agriculture dominated by artificial irrigation remains a major driver of regional economic development. Advancements in agricultural technology have contributed to the optimization and improvement of non-agricultural land and unused land in the study region. The development and exploitation of land resources has further accelerated, particularly under demographic and economic pressures (Abulizi et al., 2017; Song and Deng, 2017; Zhang et al., 2020b). Over the 41 years, the artificial nature of LULC in the region has become apparent, indicating that human activities have increasingly disturbed the land surface.

LULC change includes changes in land-use intensification and conversion, which together result in ESV changes (Song and Deng, 2017). Oases in China comprise only 3-5% of the total area of the arid regions, while supporting over 95% of population and producing more than 95% of industrial and agricultural output (Wang, 2009). The oasis ecosystem has considerable and clear ecological value in combating the stresses of the arid climate. Unused land accounted for approximately 78% of the study region from 1977 to 2017 and was always the unequivocally dominant contributor to ESV. However, increases and decreases in ESV mainly resulted from contributions from farmland, water bodies, wetland, and grassland (Table 4). There was an increase in all the ESV_f values during the study period. The ESV_f composition for the oasis ecosystems was consistent with that of the entire study region (Table 4-5, Figs. 6a, b). Farmland was the main contributor to processes associated with slight increases in ESV. The corresponding provisioning service for food production also continued to grow. The same basic pattern was observed for changes in ESV in areas for which agriculture was the main driver of development (Abulizi et al., 2017; Gashaw et al., 2018; Rukundo et al., 2018; Msofe et al., 2020). Ecosystems with high ESV, such as forests, grasslands, wetlands, and water bodies, played a decisive role in the increases and decreases in regional ESV (Li et al., 2018; Talukdar et al., 2020). The study results showed that the ESV per unit area of forest, wetland, and water systems were also significantly higher than that for farmland.

However, the aforementioned areas were small and therefore contributed less to the ESV in the study region than did farmland, which made up a larger proportion (Li et al., 2018; Talukdar et al., 2020). In other words, the high contribution of farmland to ESV came mainly from the significant expansion of its area during the study period. However, the phase analysis showed that water and wetland contributed more to the ESV than did farmland in 1997-2007 and 2007-2017 (Table 4). An LULC conversion analysis showed that farmland expanded at the expense of lands with high ESV, such as forest land, grassland, wetland, and water bodies (Table S4, Fig. 5). This unconstrained high-intensity development of land resources increased the regional ESV over the short term by increasing individual area contributions. However, this developmental overload leads to imbalances over the long term and can even ecologically degrade oases (Polasky et al., 2008; Xie et al., 2015; Msofe et al., 2020). This speculation was confirmed by the decline in the ESV of the study region for 1997-2007 under the influence of governmental immigration and relocation policies (Ma et al., 2019). In contrast, the expansion of forests, grassland, wetland, and water bodies caused ESV to increase. The 113% total ESV growth over

41 years represents the largest increase in an ESV measure in the study region since the implementation of China's Grain for Green Project (especially in 2007-2017, with a total increment of 1.14×10^9 Yuan, Table 4). Thus, there was a significant response of ESV to the drastic fluctuation in the LULC of the study region.

Arid regions are characterized by a severe scarcity of water resources and sensitive ecological environments. Ecological conservation policies, such as farmland-to-grassland policies, for arid regions can restrict the irrational exploitation of land resources and should be moderately strengthened. In addition, the continued expansion of construction land through direct human intervention has encroached on other land-use categories in the study region. Construction lands contribute significantly less to ESV than do other land-use categories (Du and Huang, 2017; Rao et al., 2018; Luo et al., 2020; Xiao et al., 2019; Talukdar et al., 2020). As a result, construction lands can decrease ESV in the study region, irrespective of conversion category. Among the 4 classes of ecosystem service functions, regulatory services contributed the most to ESV and played a key role in increases and decreases of ESV in the study region, which was generally consistent with the trends in ESV changes across the country (Song and Deng, 2017; Liu et al., 2020; Su et al., 2020; Zheng et al., 2020).

In summary, ESV in arid regions is extremely sensitive to changes in LULC. A small change in LULC can result in significant changes in ESV. Therefore, achieving synergies between regional economic development and ecological conservation requires the integration of regional socioeconomic and ecological resources and improvements in land resource quality. ESV losses to unrestrained development should be reduced. The structure and distribution of land surface resources, especially land resources, need to be fully optimized and distributed. The expansion of cultivated land should be controlled so that agricultural activities are kept at an appropriate scale. At the same time, ecological land should be protected to prevent and control the degradation caused by unreasonable utilization. To realize the optimization of agricultural economy and ecological benefits, rather than simply pursuing economic benefits and ignoring ecological benefits.

4.2 Spatial heterogeneity and mechanisms driving ESV

Exploring the spatial variation in ecosystem services and its drivers is fundamental for ecosystem service management and decision-making (Chen et al., 2020). The spatial heterogeneity of ecosystem services is influenced by the complexity of ecological processes within ecosystems and is closely related to the study scale (Hu et al., 2015). Ecosystem assessment must be performed at a scale adapted to the ecological processes or phenomena involved. Large differences were found for the same ecosystem service across different regions and at different research scales (Hou et al., 2020; Zheng et al., 2020). Spatial differentiation in the ESV of the MDSB mainly occurred in oasis ecosystems (Fig. 8). Therefore, the ESV assessment unit should reflect the fine-scale information of the oases.

A comparison in this study revealed that the grid scale more specifically represented the differentiation characteristics of the ESV in the study region than did other assessment units, capturing more detailed information on small-scale changes

(Zheng et al., 2020). This study was a quantitative analysis of the relative importance of ESV drivers in the study region, and interactions between factors were identified. Single-factor and interaction detection results showed that spatial differentiation in the ESV of the study region has resulted from interactions between several factors, among which the LA for human activities is the dominant driver. This result is consistent with those of existing studies on drivers of ecosystem services (Fang and Wang, 2013; Costanza et al., 2014; Hu et al., 2015; Tang, 2015; Luo et al., 2020; Msofe et al., 2020; Su et al., 2020). The second most important driver was the HAI. Therefore, human activities have significantly impacted the ESV in the study region. TPVI and RPCI showed an increasing trend from 1977 to 2017 in the study area (Fig. 9). Rapid socioeconomic development has accelerated the intensity of human exploitation of resources from the natural environment, forcibly converting regional natural landscapes into semi-natural (e.g., farmland) and artificial landscapes (e.g., construction land; Ma et al., 2018). At the same time, a linear increase in the population has led to a further expansion of demand for construction lands and food (Fig. 9). Within this context, large areas of non-agricultural lands have been continuously reclaimed, and regional land use has intensified. Different land cover has different ecosystem service value, and the level of service supply also has significant difference. In addition, changes in land use patterns change the spatial and temporal distribution of habitats and resources, thus affecting the structure and function of ecosystems (Liu et al., 2012; Zhang et al., 2015; Rukundo et al., 2018; Peters et al., 2019; Wu et al., 2020). Therefore, the change of land use will inevitably lead to the change of the total value of regional ecosystem services. The contributions of the landscape factors SDI and DIVISION of 11% and 8.6%, respectively, suggest that landscape pattern changes in ecosystems have also affected ecosystem functions. It is found that the change of landscape pattern affects the material cycle and energy flow process of ecosystem, and ultimately leads to the change of regional ecosystem service value through the interaction with biological and abiotic processes (Hu et al., 2020). For example, fragmentation and decentralization of landscape patches can affect the NPP of vegetation as well as the connectivity of ecological landscapes, leading to declines in the regulatory capacity, nutrient retention, and fertility of ecosystems (Mitchell et al., 2015; Huang et al., 2019). The improvement of landscape richness is helpful to enhance the value of ecosystem services (Zhang et al., 2020a). Natural factors contributed little to the ESV of the study region, except for DEM and NDVI, both contributing over 5% (Table 8).

An analysis of the driving mechanisms showed that a combination of human activities, changes in landscape patterns, and synergistic interactions between natural factors led to spatial differentiation in ESV over the study region. Therefore, future decision-making for ecosystem management should control the effect of human activities on the ecological environment. Improve the diversity of patches, reduce the degree of landscape fragmentation, improve the ecosystem service function of LULC, optimize the allocation of ecological landscape resources to achieve a win-win result for regional socioeconomic development and ecological conservation.

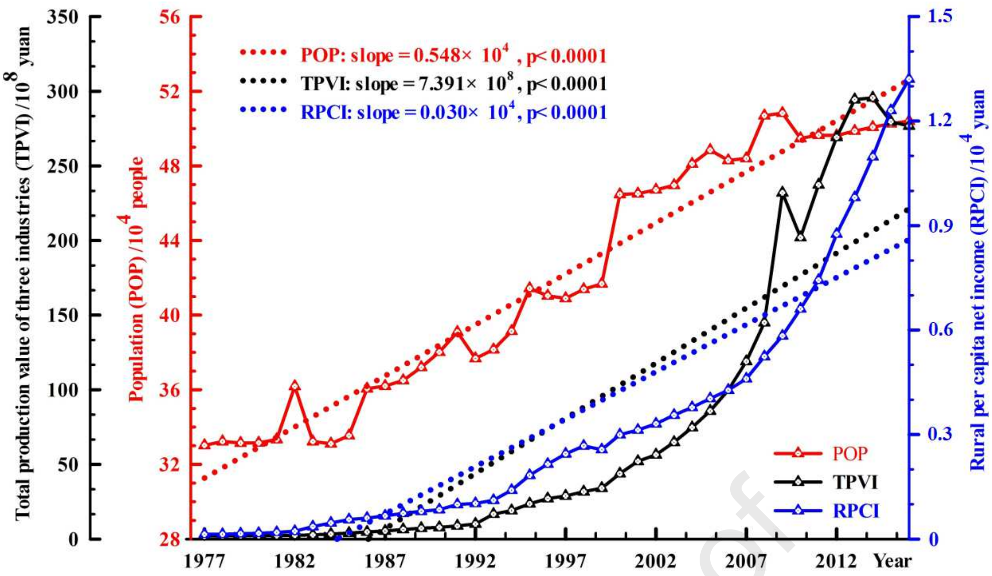

Fig. 9 Variation in total population, the total production value of 3 industries, and rural per capita net income in the MDSB.

4.3 Limitation and future work

Although this paper has corrected the value coefficient according to the actual situation of the study area, the uncertainty still exists. In this study, the equivalent coefficient of ESV per unit area was used to estimate ESV in the midstream and downstream reaches of the Shule River Basin. However, the determination of the equivalent ESV coefficient is subjective, which affects the accuracy of the ESV assessment results (Kreuter et al., 2001; Troy and Wilson, 2006; Hu et al., 2008; Liu et al., 2020; Xiao et al., 2019; Zhang et al., 2020b; Zheng et al., 2020). More realistic assessment models for the study region should be constructed to eliminate these effects. In addition, this method of estimating regional ecosystem service value based on economic value cannot quantify the value of some abstract services (such as aesthetic and cultural services). Therefore, the evaluation results cannot fully reflect the service functions and values provided by the ecosystem in the study area.

Therefore, in the future further studies, it is necessary to establish an assessment model that more comprehensively reflects the ecosystem service functions in the study area and conforms to the actual situation in the study area to eliminate these impacts.

Secondly, this paper only discusses the spatial heterogeneity of ecosystem service value and does not further discuss the trade-off and synergy relationship among various services. In the future, it is considered to introduce the ecosystem service evaluation model for system analysis. Furthermore, although the driving factors of the spatial differentiation of ecosystem service value in the study area are quantitatively analysed in this paper, the policy factors are difficult to be quantified, so the quantitative analysis is not carried out. In the future, it is necessary to seek appropriate policy proxy indicators and incorporate them into the driving factor index system.

5. Conclusions

This study utilized the benefit transfer method to assess the ESV of the midstream and downstream regions of the Shule River Basin (MDSB), and the spatiotemporal distribution of ESV was analysed accordingly. Then, contributions of factors driving ESV were quantified using Geographical detector model. The main results showed that the LULC structure in the study region was stable overall and that changes in LULC were concentrated in the oases and peripheral regions, which were characterized by intensive human activities. Farmland and construction land underwent sustained expansion over the 41-year study period. There was little variation in the total areas of grassland or desertified land, but there was substantial conversion within these 2 categories between lands of different levels of development, with an overall positive development trend, indicating a general improvement in the regional ecological environment. The total ESV for the study area increased slightly over the investigated period. The services provided by oasis ecosystems dominated the fluctuations in the ESV throughout the study region. Regulatory services represented the greatest contribution to ESV among all services. The ESV of the study region exhibited a strong positive spatial autocorrelation, with aggregations of high and low values across spatial scales. Synergized interactions among human activities, changes in landscape patterns, and natural factors produced the spatial variation in the ESV of the study region. The main driver of differentiation was the impact of human activities, reflected by the land-use intensity and human activity indices.

ACKNOWLEDGEMENTS

We would like to express our sincere gratitude to the editors and reviewers who have put considerable time and effort into their comments on this paper. This work was supported by the National Natural Science Foundation of China (Grant No. 41671188).

REFERENCES

Abulizi, A., Yang, Y. G., Mamat, Z., Luo, J. H., Abdulslam, D., Xu, Z. L., ... Halik, W., 2017.

Land-use change and its effects in Charchan Oasis, Xinjiang, China. Land Degrad. Dev. 28, 106-115. https://doi.org/10.1002/ldr.2530.

Anselin, L., Cho, W.K.T., 2002. Spatial effects and ecological inference. Polit. Anal. 10 (3), 276-297. https://doi.org/10.1093/pan/10.3.276.

Cao, B., Kong, X. L., Wang, Y. X., Liu, H., Pei, H. W., & Shen, Y. J., 2021. Response of Vegetation Cover Change to Drought at Different Time-scales in the Beijing-Tianjin Sandstorm Source Region, China. Chin. Geogr. Sci. 31, 491-505. https://doi.org/10.1007/s11769-021-1206-8.

Chang, G.Y., Zhang, W.X., 2014. Ecological civilization-based rethinking of large-scale immigration and land development along Shule River. J. Lanzhou Univ.: Natural Sciences. 50, 405-409 (in Chinese). https://doi.org/10.13885/j.issn.0455-2059.2014.03.017.

Chen, H. J., 2021. The ecosystem service value of maintaining and expanding terrestrial protected areas in China. Sci. Total Environ., 781, 146768. https://doi.org/10.1016/j.scitotenv.2021.146768.

Chen, T. Q., Feng, Z., Zhao, H. F., Wu, K. N., 2020. Identification of ecosystem service bundles and driving factors in Beijing and its surrounding areas. Sci. Total Environ.,711, 134687. https://doi.org/10.1016/j.scitotenv.2019.134687.

Chen, X., Bai, J., Li, X., Luo, G., Li, J., Li, B. L., 2013. Changes in land use/land cover and ecosystem services in Central Asia during 1990–2009. Current Opinion in Environmental Sustainability, 5(1), 116-127. https://doi.org/10.1016/j.cosust.2012.12.005.

Costanza, R., Derge, R., de Groot, R., Farber, S., Grasso, M., Hannon, B., ... van den Belt, M., 1997. The value of the world's ecosystem services and natural capital. Nature, 387, 253-260.

Costanza, R., Groot, R. D., Sutton, P., Ploeg, S. V. D., Anderson, S. J., Kubiszewski, I., ... Turner, R. K., 2014. Changes in the global value of ecosystem services. Glob. Environ. Change. 6, 152-158. https://doi.org/10.1016/j.gloenvcha.2014.04.002.

Damtea, W., Kim, D., & Im, S., 2020. Spatiotemporal analysis of land cover changes in the Chemoga Basin, Ethiopia, using Landsat and Google Earth Images. Sustainability, 12. https://doi:10.3390/su12093607.

Ding, Y., Zhang, M., Qian, X., Li, C., Chen, S., Wang, W., 2019. Using the geographical detector technique to explore the impact of socioeconomic factors on pm2.5 concentrations in China. J. Clean Prod., 211(FEB.20), 1480-1490. https://doi.org/10.1016/j.jclepro.2018.11.159.

Du, X. J., Huang, Z. H., 2017. Ecological and environmental effects of land use change in rapid urbanization: the case of Hangzhou, China. Ecol. Indic., 81, 243-251. http://dx.doi.org/10.1016/j.ecolind.2017.05.040.

ESRI, 2013. ESRI Desktop 2013, Desktop 2013 ed. Environmental Systems Research Institute: Redlands, CA, USA.

Fang, C., Wang, J., 2013. A theoretical analysis of interactive coercing effects between urbanization and eco-environment. Chin. Geogr. Sci. 23, 147-162. https://doi.org/10.1007/s11769-013-0602-2.

Fu B. J., 2013. Ecosystem Services and Ecological Security. Higher Education Press, Beijing (In Chinese).

Fu, B. J., Stafford-Smith, M., & Fu, C., 2021. Editorial overview: dryland social-ecological systems in changing environments. Curr. Opin. Environ. Sustain., 48, A1-A5. https://doi.org/10.1016/j.cosust.2021.03.001.

Gashaw, T., Tulu, T., Argaw, M., Worqlul, A. W., Tolessa, T., Kindu, M., 2018. Estimating the impacts of land use/land cover changes on Ecosystem Service Values: The case of the Andassa watershed in the Upper Blue Nile basin of Ethiopia. Ecosyst. Serv., 31, 219-228. https://doi.org/10.1016/j.ecoser.2018.05.001.

Gong, S., Xiao, Y., Xiao, Y., et al., 2017. Driving forces and their effects on water conservation services in forest ecosystems in China. Chin. Geogr. Sci. 27 (2), 216-228. http://dx.doi.org/10.1007/s11769-017-0860-3.

Good, I.J., 1983. The philosophy of exploratory data analysis. Philos. Sci. 50, 283-295.

Guan, Q.Y., Yang, Li. Q., Pan, N. H., Lin, J. K., Xu, C. Q., Wang, F. F., Liu, Z. Y., 2018. Greening and Browning of the Hexi Corridor in Northwest China: Spatial Patterns and Responses to Climatic Variability and Anthropogenic Drivers. Remote Sens. 10, 1270. http://dx.doi.org/10.3390/rs10081270.

Han, J. J., Wang, J. P., Chen, L., Xiang, J. X., Ling, Z. Y., Li, Q. K., Wang. E. L., 2021. Driving factors of desertification in Qaidam Basin, China: An 18-year analysis using the geographic detector model. Ecol. Ind. 124, 107404. https://doi.org/10.1016/j.ecolind.2021.107404.

Hao, L., Pan, C., Fang, D., Zhang, X. Y., Zhou, D. C., Liu, P. L., ... Sun, G., 2018. Quantifying the effects of overgrazing on mountainous watershed vegetation dynamics under a changing climate. Sci. Total Environ., 639, 1408-1420. http://dx.doi.org/10.1016/j.scitotenv.2018.05.224.

Hao, R. F., Yu, D. Y., Liu, Y. P., Liu, Y., Qiao, J. M., Wang, X., ... Du J. S., 2016. Impacts of changes in climate and landscape pattern on ecosystem services. Sci. Total Environ. 579, 718-728. http://dx.doi.org/10.1016/j.scitotenv.2016.11.036.

He, C.Y., Li, J.W., Zhang, X.L., Liu, Z.F., Zhang, D., 2017. Will rapid urban expansion in the drylands of northern China continue: a scenario analysis based on the Land Use Scenario Dynamics-urban model and the Shared Socioeconomic Pathways. J. Cleaner Prod. 165, 57-69. https://doi.org/10.1016/j.jclepro.2017.07.018.

Hou, M. J., Ge, J., Gao, J. L., Meng, B. P., Li, Y. C.,...Liang, T. G., 2020. Ecological Risk Assessment and Impact Factor Analysis of Alpine Wetland Ecosystem Based on LUCC and Boosted Regression Tree on the Zoige Plateau, China. Remote Sens. 12, 368. http://dx.doi.org/doi:10.3390/rs12030368.

Hu, H., Liu, W., Cao, M., 2008. Impact of land use and land cover changes on ecosystem services in Menglun, Xishuangbanna, Southwest China. Environ. Monit. Assess. 146, 147-156. https://doi.org/10.1007/s10661-007-0067-7.

Hu, X. S., Hong, W., Qiu, R. Z., Hong, T., Chen, C., Wu, C. Z., 2015. Geographic variations of ecosystem service intensity in Fuzhou city, China. Sci. Total Environ. 512-513, 215-226. https://doi.org/10.1016/j.scitotenv.2015.01.035.

Huang, C. B., Huang, X., Peng, C. H., Zhou, Z. X., Teng, M. J., & Wang, P. C., 2019. Land use/cover change in the three gorges reservoir area, china: reconciling the land use conflicts between development and protection. Catena, 175, 388-399. https://doi.org/10.1016/j.catena.2019.01.002.

Huang, J. P., Yu, H. P., Dai, A. G., Wei, Y., Kang, L. T. 2017. Drylands face potential threat under 2° C global warming target. Nat. Clim. Change, https://doi.org/10.1038/nclimate3275.

Huang, M, Y., Yue, W. Z., Fang, B., Feng, S. R., 2019. Scale response characteristics and geographic exploration mechanism of spatial differentiation of ecosystem service values in Dabie Mountain area, central China from 1970 to 2015. J. Geogr. Sci. 74 (9), 1904-1920. https://doi.org/10.11821/dlxb201909015.

Kareiva, Peter, Wennergren, Uno., 1995. Connecting landscape patterns to ecosystem and population processes. Nature. 373, 299-302. http://dx.doi.org/10.1038/373299a0.

Kim, I., Arnhold, S., 2018. Mapping environmental land use conflict potentials and ecosystem services in agricultural watersheds. Sci. Total Environ. 630, 827-838. http://dx.doi.org/10.1016/j.scitotenv.2018.02.176.

Kindu, M., Schneider, T., Teketay, D., Knoke, T., 2016. Changes of ecosystem service values in response to land use/land cover dynamics in munessa-shashemene landscape of the ethiopian highlands. Sci. Total Environ., 547, 137-147. http://dx.doi.org/10.1016/j.scitotenv.2015.12.127.

King, D.M., Mazzotta, M.J., Markowitz, 2000. Ecosystem valuation. Available: http://www.ecosystemvaluation.org/default.htm (Accessed 27 July 2020).

Kreuter, U. P., Harris, H. G., Matlock, M. D., Lacey, R. E., 2001. Change in ecosystem service values in the San Antonio area, Texas. Ecol. Econ., 39, 333-346. http://dx.doi.org/10.1016/S0921-8009(01)00250-6.

Kumari, M., Sarma, K., Sharma, R., 2019. Using Moran's I and GIS to study the spatial pattern of land surface temperature in relation to land use/cover around a thermal power plant in Singrauli district, Madhya Pradesh, India. Remote. Sens. Appl. 15, 100239. https://doi.org/10.1016/j.rsase.2019.100239.

Leh, M. D., Matlock, M. D., Cummings, E. C., Nalley, L. L., 2013. Quantifying and mapping multiple ecosystem services change in West Africa. Agriculture, Ecosystems and Environment, 165, 6-18. https://doi.org/10.1016/j.agee.2012.12.001.

Li, F., Zhang, S. W., Yang, J. C., Chang, L. P., Yang, H. J., Bu, K., 2018. Effects of land use change on ecosystem services value in West Jilin since the Reform and Opening of China. Ecosyst. Serv. 31, 12-20. https://doi.org/10.1016/j.ecoser.2018.03.009.

Li, J.; Gong, J.; Guldmann, J.-M.; Li, S.; Zhu, J., 2020. Carbon Dynamics in the Northeastern Qinghai–Tibetan Plateau from 1990 to 2030 Using Landsat Land Use/Cover Change Data. Remote Sens. 12, 528. https://doi.org/10.3390/rs12030528.

Lin, J. K., Guan, Q. Y., Pan, N. H., Zhao, R., Yang, L. Q., & Xu, C.Q., 2020. Spatiotemporal Variations and Driving Factors of the Potential Wind Erosion Rate in the Hexi Region. Land Degrad. Dev., https://doi.org/10.1002/ldr.3702.

Lindenmayer, D. B., Franklin, J. F., 2010. Managing stand structure as part of ecologically sustainable forest management in Australian Mountain Ash Forests. Conserv. Biol. 11 (5), 1053-1068. https://doi.org/10.1046/j.1523-1739.1997.96150.x.

Liu, C., Zhang, F., Johnson, V. C., Duan, P., & Kung, H. T., 2021. Spatio-temporal variation of oasis landscape pattern in arid area: human or natural driving? Ecol. Ind., 125(1), 107495. https://doi.org/10.1016/j.ecolind.2021.107495.

Liu, J. Y., Zhang, Z. X., Xu, X. L., Kuang, W. H., Zhou, W. C., Zhang, S.W., ... Jiang N., 2010. Spatial patterns and driving forces of land use change in China during the early 21st century. J. Geogr. Sci. 20, 483-494. http://dx.doi.org/10.1007/s11442-010-0483-4.

Liu, Y. B., Hou, X. Y., Li, X. W., Song, B. Y., Wang, C., 2020. Assessing and predicting changes in ecosystem service values based on land use/cover change in the Bohai Rim coastal zone. Ecol. Indic. 111, 106004. https://doi.org/10.1016/j.ecolind.2019.106004.

Liu, Y., Li, J., Zhang, H., 2012. An ecosystem service valuation of land use change in Taiyuan city, China. Ecol. Model. 225, 127-132. http://dx.doi.org/10.1016/j.ecolmodel.2011.11.017.

Lü, Y. H., Ma, Z. M., Zhao, Z. J., Sun, F. X., Fu, B. J., 2014. Effects of land use change on soil carbon storage and water consumption in an Oasis-Desert Ecotone. Environ. Manage., 53, 1066-1076. https://doi.org/10.1007/s00267-014-0262-6.

Luo, Q. L., Zhou, J. F., Li, Z. G., Yu, B, L., 2020. Spatial differences of ecosystem services and their driving factors: A comparation analysis among three urban agglomerations in China's Yangtze River Economic Belt. Sci. Total Environ., 725, 138452. https://doi.org/10.1016/j.scitotenv.2020.138452.

Ma, L. B., Cheng, W. J., Bo, J., Li, X. Y., Gu, Y., 2018. Spatio-temporal variation of land-use intensity from a multi-perspective—taking the middle and lower reaches of Shule River Basin in China as an example. Sustainability. 10, 771. https://doi.org/10.3390/su10030771.

Ma, L. B., Bo, J., Li, X. Y., Fang, F., Cheng, W. J., 2019. Identifying key landscape pattern indices influencing the ecological security of inland river basin: the middle and lower reaches of shule river basin as an example. Sci. Total Environ., 674 (JUL.15), 424-438. https://doi.org/10.1016/j.scitotenv.2019.04.107.

Mahmoud, S. H., Gan, T. Y., 2018. Impact of anthropogenic climate change and human activities on environment and ecosystem services in arid regions. Sci. Total Environ. 633, 1329-1344. http://dx.doi.org/10.1016/j.scitotenv.2018.03.290.

Millennium Ecosystem Assessment (MEA), 2005. Ecosystems and Human Well-Being:Synthesis. Island Press, Washington DC.

Mitchell, M.G.E., Suarez-Castro, A.F., Martinez-Harms, M., Maron, M., McAlpine, C., Gaston, K.J., Johansen, K., Rhodes, J.R., 2015. Reframing landscape fragmentation’s effects on ecosystem services. Trends Ecol. Evol. 30 (4), 190-198. https://doi.org/10.1016/j.tree.2015.01.011.

Moran, 1950. Notes on Continuous Stochastic Phenomena. Biometrika, 37, 17-23. https://doi.org/10.1093/biomet/37.1-2.17.

Morshed, S. R., Fattah, M. A., Haque, M. N., & Morshed, S. Y., 2021. Future ecosystem service value modeling with land cover dynamics by using machine learning based Artificial Neural

Network model for Jashore city, Bangladesh. Physics and Chemistry of the Earth Parts A/B/C (11), 103021. https://doi.org/10.1016/j.pce.2021.103021.

Msofe, N. K., Sheng, L. X., Li, Z. X., Lyimo, J., 2020. Impact of Land Use/Cover Change on Ecosystem Service Values in the Kilombero Valley Floodplain, Southeastern Tanzania. Forests. 11, 109. https://doi.org/10.3390/f11010109.

Nagendra, H., Mairota, P., Marangi, C., Lucas, R., Dimopoulos, P., Honrado, J.P., Niphadkar, M., Mücher, C.A., Tomaselli, V., & Panitsa, M., 2015. Satellite Earth observation data to identify anthropogenic pressures in selected protected areas. Int. J. Appl. Earth Obs. Geoinf. 37, 124–132. https://doi.org/10.1016/j.jag.2014.10.010.

Pan, J. H., Wei, S. M., & Li, Z., 2020. Spatiotemporal pattern of trade-offs and synergistic relationships among multiple ecosystem services in an arid inland river basin in NW China. Ecol. Ind., 114. https://doi.org/10.1016/j.ecolind.2020.106345.

Peters, M. K., Hemp, A., Appelhans, T. Becker, J. N., Behler, C., Classen, A.,...Steffan-Dewenter, I., 2019. Climate–land-use interactions shape tropical mountain biodiversity and ecosystem functions. Nature. 568, 88-92. https://doi.org/10.1038/s41586-019-1048-z.

Polasky, S., Nelson, E., Camm, J., Csuti, B., Fackler, P.,...Tobalske, C., 2008. Where to put things? Spatial land management to sustain biodiversity and economic returns. Biol. Conserv. 141 (6), 1505-1524. https://doi.org/10.1016/j.biocon.2008.03.022.

Polasky, S., Nelson, E., Pennington, D., Johnson, K.A., 2011. The impact of land-use change on ecosystem services, biodiversity and returns to landowners: a case study in the State of Minnesota. Environ. Resour. Econ. 48, 219-242. https://doi.org/10.1007/s10640-010-9407-0.

Qiao, P., W, Yang, S. C., Tong, M. L., Chen, B., Dong, N., 2019. Quantitative analysis of the factors influencing spatial distribution of soil heavy metals based on geographical detector, Sci. Total Environ., 664, 392-413. https://doi.org/10.1016/j.scitotenv.2019.01.310.

Rao, Y. X., Zhou, M., Ou, G. L., Dai, D. Y., Zhang, L., Zhang, Z., ... Yang, C., 2018. Integrating ecosystem services value for sustainable land-use management in Semi-Arid Region. J. Clean Prod. 186, 662-672. http://dx.doi.org/10.1016/j.jclepro.2018.03.119.

Redo, D.J., Aide, T.M., Clark, M.L., Andrade-Núñez, M.J., 2012. Impacts of internal and external policies on land change in Uruguay, 2001–2009. Environ. Conserv. 39 (02), 122-131. https://doi.org/10.1016/j.ecolind.2019.105752.

Rukundo, E., Liu, S. L., Dong, Y. H., Rutebuka, E., Asamoah, E. F., Xu, J. W., Wu, X., 2018. Spatio-temporal dynamics of critical ecosystem services in response to agricultural expansion in Rwanda, east Africa. Ecol. Indic. 89, 696-705. http://dx.doi.org/10.1016/j.ecolind.2018.02.032.

Shi, L., Halik, M., Mamat, Z., Tayierjiang, A., & Welp, M., 2021. Spatiotemporal investigation of the interactive coercing relationship between urbanization and ecosystem services in arid north）estern China. Land Degrad. Dev., 1-16. https://doi.org/10.1002/ldr.3946.

Song, F., Su, F. L., Mi, C. X., & Sun, D., 2021. Analysis of driving forces on wetland ecosystem services value change: A case in Northeast China. Sci. Total Environ., 751, 141778. https://doi.org/10.1016/j.scitotenv.2020.141778.

Song, W., Deng, X. Z., 2017. Land-use/land-cover change and ecosystem service provision in China. Sci. Total Environ. 576, 705-719. http://dx.doi.org/10.1016/j.scitotenv.2016.07.078.

Su, K., Wei, D. Z., Lin, W. X., 2020. Evaluation of ecosystem services value and its implications for policy making in China – A case study of Fujian province. Ecol. Indic. 108, 105752. https://doi.org/10.1016/j.ecolind.2019.105752.

Symanzik, J., 2013. Exploratory spatial data analysis. Handbook of Regional Science. Springer, pp. 1295-2310.

Talukdar, S., Singha, P., Shahfahad, Mahato, S., Praveen, B., Rahman, A., 2020. Dynamics of ecosystem services (ESs) in response to land use land cover (LU/LC) changes in the lower Gangetic plain of India. Ecol. Indic. 112, 106-121. http://dx.doi.org/10.1016/j.ecolind.2020.106121.

Tang, Z., 2015. An integrated approach to evaluating the coupling coordination between tourism and the environment. Tour. Manag. 46, 1 1-19. https://doi.org/10.1016/j.tourman.2014.06.001.

Tolessa, T., Senbeta, F., Kidane, M., 2017. The impact of land use/land cover change on ecosystem services in the central highlands of Ethiopia. Ecosyst. Serv. 23, 47-54. http://dx.doi.org/10.1016/j.ecoser.2016.11.010.

Troy, A., Wilson, M.A., 2006. Mapping ecosystem services: Practical challenges and opportunities in linking GIS and value transfer. Ecol. Econ. 60, 435-449. http://dx.doi.org/10.1016/j.ecolecon.2006.04.007

Wang, C. D., Wang, Y. T., Wang, R.Q., Zheng, P. M., 2018. Modeling and evaluating land-use/land-cover change for urban planning and sustainability: a case study of Dongying city, China. J. Clean Prod. 172, 1529-1534. http://dx.doi.org/10.1016/j.jclepro.2017.10.294.

Wang, J. F., Li, X. H., Christakos, G., Liao, Y. L., Zhang, T., Xue, G., Zheng, X. Y., 2010. Geographical detectors-based health risk assessment and its application in the neural tube defects study of the Heshun Region, China. Int. J. Geogr. Inf. Sci. 24, 107-127. https://doi.org/10.1080/13658810802443457.

Wang, J. F., Zhang, T. L., Fu, B. J., 2016. A measure of spatial stratified heterogeneity. Ecol. Indic., 67, 250-256. https://doi.org/10.1016/j.ecolind.2016.02.052.

Wang, J. P., Mwangetti, A., Ma, Y. X., 2020. Study on the Change data of land use and Ecological Service value in Yerqiang River Basin from 1978 to 2018. Journal of Global change data ＆Discovery. 4, 75-85. https://doi.org/10.3974/geodp.2020.01.11.

Wang, S., X, Wu, B., & Yang, P. N., 2014. Assessing the change in land use and ecosystem services in an oasis agricultural region of Yanqi Basin, Northwest China. Environ. Monit. Assess., 186, 8343-8357. https://doi.org/10.1007/s10661-014-4009-x.

Wang, T., 2009. Review and prospect of research on oasification and desertification in Arid Regions. Journal of Desert Research, 29, 1-9 (In Chinese). http://dx.doi.org/ 10.1007/978-1-4020-9623-55.

Wang, T., Yan, C. Z., Song, X., Li, S., 2013. Landsat images reveal trends in the aeolian desertification in a source area for sand and dust storms in China's Alashan Plateau (1975-2007). Land Degrad. Dev., 24, 422-429. https://doi.org/10.1002/ldr.1138.

Wang, Q. Z., Guan, Q. Y., Lin, J. K., Luo, H. P., & Ma, Y. R., 2021. Simulating land use/land cover change in an arid region with the coupling models. Ecol. Indic. 122, 107231. https://doi.org/10.1016/j.ecolind.2020.107231.

Wang, X. C., Dong, X. B., Liu, H. M., Wei, H. J., Fan, W. G., Lu, N., ... Xing K. X., 2017. Linking land use change, ecosystem services and human well-being: a case study of the Manas River Basin of Xinjiang, China. Ecosyst. Serv. 27, 113-123. http://dx.doi.org/10.1016/j.ecoser.2017.08.013.

Wang, Y ., Pan, J. H ., 2019. Building ecological security patterns based on ecosystem services value reconstruction in an arid inland basin: A case study in Ganzhou District, NW China. J. Cleaner Prod., 241, 118337. https://doi.org/10.1016/j.jclepro.2019.1 18337.

Wei, H. J., Liu, H. M., Xu, Z. H., Ren, J. H., Lu, N. C., Fan, W., ... Dong, X. B., 2018. Linking ecosystem services supply, social demand and human well-being in a typical mountain–oasis–desert area, Xinjiang, China. Ecosyst. Serv., 31, 44-57. https://doi.org/10.1016/j.ecoser.2018.03.012.

Wei, J., 2017. Ecosystem services research in China: a critical review. Ecosyst. Serv., 26, 10-16. https://doi.org/10.1016/j.ecoser.2017.05.012.

Wu, C. Y., Chen, B. W., Huang, X. J., Wei, Y. H. D., 2020. Effect of land-use change and optimization on the ecosystem service values of Jiangsu province, China. Ecol. Ind. 117, 106507. https://doi.org/10.1016/j.ecolind.2020.106507.

Xiao, R., Lin, M., Fei, X. F., Li, Y. S., Zhang Z. H., Meng, Q. X., 2019. Exploring the interactive coercing relationship between urbanization and ecosystem service value in the Shanghai–Hangzhou Bay Metropolitan Region. J. Clean Prod., 253, 119803. https://doi.org/10.1016/j.jclepro.2019.1 19803.

Xie, G. D., Zhang, Y. L., Lu, C. X., Zheng, D., Cheng, S. K., 2001. Journal of Natural Resources, 16, 47-53 (In Chinese). https://doi.org/10.3321/j.issn:1000-3037.2001.01.009.

Xie, G. D., Lu, Chun. Xia., Leng, Y. F., Zheng, D., Li, S. C., 2003. Ecological assets valuation of the Tibetan Plateau. Journal of Natural Resources, 18, 189-196 (In Chinese). https://doi.org/10.3321/j.issn:1000-3037.2003.02.010.

Xie, G. D., Zhang, C. X., Zhang, L. M., Chen, W. H., Li, S. M., 2015. Improvement of the evaluation method for ecosystem service value based on per unit area. Journal of Natural Resources, 30 (08), 1243-1254 (In Chinese). https://doi.org/10.11849/zrzyxb.2015.08.001.

Xie, G. D., Zhen, L., Lu, C. X., Xiao, Y., Chen, C., 2008. Expert knowledge-based valuation method of ecosystem services in China. Journal of Natural Resources, 23, 911-919 (In Chinese). http://dx.doi.org/10.11849/zrzyxb.2008.05.019/.

Xu, X. B., Yang, G. S., Tan, Y., Zhuang, Q. L., Li, H. P., Wan, R. R., Zhang J., 2016. Ecological risk assessment of ecosystem services in the Taihu Lake Basin of China from 1985 to 2020. Sci. Total Environ. 554-555, 7-16. http://dx.doi.org/10.1016/j.scitotenv.2016.02.120.

Xu, X. L., Liu, J. Y., Zhang, S. W., Li, R. D., Yan, C. Z., Wu, S. X., 2018. Remote sensing monitoring dataset of land use and land cover in China. DOI:10.12078/2018070201. http://www.resdc.cn/DOI.

Yan, C. Z., Wang, T., Han, Z. W., Qie, Y., F., 2007. Surveying sandy deserts and desertified lands in north-western China by remote sensing. Int. J. Remote Sens. 28, 3603-3618. https://doi.org/10.1080/01431160601024218.

Yang, Q., Chen, W. Y., Xu, Y. F., Lv, X. D., Zhang, M., Jiang, H., 2018. Polyphyllin I modulates MALAT1/STAT3 signaling to induce apoptosis in gefitinib-resistant non-small cell lung cancer. Toxicol. Appl. Pharmacol. 356, 1-7. https://doi.org/10.1016/j.taap.2018.07.031.

Yushanjiang, A., Zhang, F., Yu, H. Y., Kung, H. T., 2018. Quantifying the spatial correlations between landscape pattern and ecosystem service value: a case study in Ebinur Lake Basin, Xinjiang, China. Ecol. Eng., 113, 94-104. http://dx.doi.org/10.1016/j.ecoleng.2018.02.005.

Zhan, J., Zhang, F., Chu, X., Liu, W., Zhang, Y., 2019. Ecosystem services assessment based on emergy accounting in Chongming Island, Eastern China. Ecol. Ind. 105, 464-473. https://doi.org/10.1016/j.ecolind.2018.04.015.

Zhang, F., Tiyip, T., Feng, Z. D., Kung, H., Johnson, V. C., Ding, J. L., ...Tashpolat, N., 2015. Spatio-temporal patterns of land use/cover changes over the past 20 years in the middle reaches of the Tarim river, Xinjiang, China. Land Degrad. Dev. 26, 284-299. https://doi.org/10.1002/ldr.2206.

Zhang, J., Qu, M., Wang, C., Zhao, J., Cao, Y., 2020a. Quantifying landscape pattern and ecosystem service value changes: A case study at the county level in the Chinese LoessPlateau. Glob. Ecol. Conserv., 23, e01110. https://doi.org/10.1016/j.gecco.2020.e01110.

Zhang, Z. P., Xia, F. Q., Yang, D. G., Huo, J. W., Chen, H. X., 2020b. Spatiotemporal characteristics in ecosystem service value and its interaction with human activities in Xinjiang, China. Ecol. Indic. 110, 105826. https://doi.org/10.1016/j.ecolind.2019.105826.

Zheng, D. F., Wang, Y. H., Hao, S., Xu, W. J., Lv, L. T., Yu, S., 2020. Spatial-temporal variation and tradeoffs/synergies analysis on multiple ecosystem services: a case study in the Three-River Headwaters region of China. Ecol. Indic. 116, 106494. https://doi.org/10.1016/j.ecolind.2020.106494.

Table 1 ESV per unit are of different LULC types in the MDSB (Yuan/hm^2) (2015 prices)

Service type categories	Service type subcategories	FoL	GL	FaL	WL	WA	UL	Total
Provision services	FP	646.06	1367.68	1957.75	704.79	1037.61	39.16	5753.05
	RMP	5834.11	21.71	763.52	469.86	685.21	78.31	7852.73
Regulatory services	GR	8457.50	162.82	1409.58	4718.19	998.45	117.47	15864.01
	CR	7968.06	893.70	1899.02	26527.57	4032.97	254.51	41575.82
	HR	8007.21	806.86	1507.47	26312.21	36747.04	137.04	73517.84
	WD	3367.34	2532.74	2721.28	28191.66	29072.65	509.02	66394.68
Support services	SC	7870.17	589.77	2877.90	3895.93	802.68	332.82	16369.26
	BP	8829.47	1005.86	1996.91	7224.11	6715.10	783.10	26554.55
Cultural services	PAL	4072.13	325.64	332.82	9181.87	8692.43	469.86	23074.74
	Total	55052.04	7706.78	15466.3	107226.2	88784.14	2721.3	276956.68

Notes: Provision services--Food production (FP) and Raw material production (RMP); Regulatory services--Gas regulation (GR), Climate regulation (CR), Hydrological regulation (HR), and Waste decomposition (WD); Support services--Soil conservation (SC) and Biodiversity protection (BP); and Cultural services (Provide aesthetic landscape--PAL).

Table 2 Data sources and processing

	Driving factors	Sources	Processing
Nature factors	Temperature (Tem)	http://data.cma.cn/	Anusplin interpolation model
	Precipitation (Pre)		
	Elevation		
	Slope		
	Net Primary Productivity (NPP)	https://data.tpdc.ac.cn	
	Normalized Difference Vegetation Index (NDVI)		ArcGIS Spatial analysis function
Human factors	Gross Domestic Product (GDP)	http://www.resdc.cn/	
	Population (POP)		
	Road density	http://www.webmap.cn/	
	Human activity intensity (HAI)	Xu et al., 2016	$HAI = \frac{Acle}{A} \times 100\%$ $Acle = \sum_{i=1}^{m} (ALi \bullet CIi)$
	Land use intensity (LA)	Zhuang and Liu, 1997	$La = 100 \times \sum_{i=1}^{n} Ai \times Ci$
Landscape pattern factors	Landscape Division Index (DIVISION)	LULC data	Fragstats software 4.2
	Shannon's Diversity Index (SDI)		
	Mean Shape Index (MSI)		
Statistic data	total population	National/Local Bureau of Statistics	
	the total production value of three industries		
	rural per capita net income		

Table 3 Area and dynamic degrees (K) of various LULC types in the MDSB from 1977 to 2017

LULC type	Area (km^2)					K (%)				
	1977	1987	1997	2007	2017	1977-1987	1987-1997	1997-2007	2007-2017	1977-2017
FaL	1323.3	1340.5	1416.2	1781.3	1949.1	0.13	0.56	2.58	0.94	1.18
GL	6787.4	6782	6829.4	6417.6	6556.4	-0.01	0.07	-0.60	0.22	-0.09
FoL	11	10.2	8.1	6.9	7.4	-0.68	-2.05	-1.50	0.74	-0.81
SaL	753.5	758.4	754	592.3	511	0.07	-0.06	-2.14	-1.37	-0.80
CL	109.4	122.5	137.2	134.4	167.1	1.20	1.20	-0.21	2.44	1.32
WB	358.9	362.2	366.8	331.9	409.2	0.09	0.12	-0.95	2.33	0.35
DL	7033.5	7044.4	7052.2	6607.2	6584.8	0.02	0.01	-0.63	-0.03	-0.16
BL	21769.7	21727	21582.8	22275	21961.9	-0.02	-0.07	0.32	-0.14	0.02

Table 4 Change in ESV in study area from 1977 to 2017 ($\times 10^6$ yuan)

	Year	FoL	GL	FaL	WL	WA	UL	Total
Ecosystem services value	1977	60.34	5230.91	2046.71	2722.17	932.06	8043.18	19035.36
	1987	56.21	5226.74	2073.24	2800.43	897.34	8035.88	19089.83
	1997	44.70	5263.23	2190.35	2803.96	934.54	7997.53	19234.32
	2007	37.99	4945.87	2755.05	1158.04	1988.14	8020.82	18905.92
	2017	40.79	5052.87	3014.56	2304.29	1724.99	7907.41	20044.91
Change (%)	1977-2007	-37	-5	+35	-57	+113	0.00	-1
	2007-2017	+7	+2	+9	+99	-13	-1	+6
	1977-2017	-32	-3	+47	-15	+85	-2	+5

Notes: “+” means increase and “-” means decrease.

Table 5 The values of individual ecosystem functions (ESV_f) in the study area from 1977 to 2017 ($\times 10^6$ yuan)

		1977		1987		1997		2007		2017	
Service type categories	Service type subcategories		%		%		%		%		%
Provision services	FP	1332.60	7.00	1335.17	6.99	1356.25	7.05	1370.08	7.35	1427.86	7.12
	RMP	372.75	1.96	373.47	1.96	377.34	1.96	403.17	2.16	418.34	2.09
Regulatory services	GR	783.77	4.12	788.20	4.13	796.80	4.14	778.00	4.17	849.88	4.24
	CR	2334.66	12.26	2353.94	12.33	2369.87	12.32	2032.31	10.90	2349.96	11.72
	HR	2214.73	11.63	2220.75	11.63	2248.64	11.69	2193.92	11.77	2506.39	12.50
	WD	4608.27	24.21	4619.16	24.20	4656.99	24.21	4482.10	24.04	4843.25	24.16
Support services	SC	1880.80	9.88	1886.46	9.88	1905.18	9.91	1935.20	10.38	2019.86	10.0
	BP	3525.13	18.52	3527.90	18.48	3537.95	18.39	3523.96	18.90	3616.47	18.04
Cultural services	PAL	1982.63	10.42	1984.77	10.40	1985.30	10.32	1924.02	10.32	2012.90	10.04
	Total	19035.4	100	19089.8	100	19234.3	100	18642.8	100	20044.9	100

Definitions of acronyms given in Table 1, and % represents the percentage of ESV_f in the total ESV.

Table 6 The results of a sensitivity test (*CS*) for ESV in the MDSB

Time	FoL	GL	FaL	WL	WA	UL
1977	0.010	0.550	0.215	0.286	0.098	0.845
1987	0.009	0.548	0.217	0.293	0.094	0.842
1997	0.007	0.547	0.228	0.292	0.097	0.823
2007	0.006	0.523	0.291	0.123	0.210	0.848
2017	0.010	0.504	0.301	0.230	0.172	0.789

Table 7 Global Moran's I of ESV in the MDSB, 1977-2017

Year	1977	1987	1997	2007	2017
Moran's I	0.637	0.641	0.642	0.627	0.672
Z (I)	86.519	87.035	87.004	89.401	97.246
P-value	0.001	0.001	0.001	0.001	0.001

Table 8 The contributions (q statistics) of various factors to differences in ESV

	Variables	q-Statistic	P-value
X_1	Tem	0.031	0.000
X_2	Pre	0.020	0.000
X_3	Elevation	0.067	0.000
X_4	Slope	0.012	0.000
X_5	NPP	0.019	0.000
X_6	NDVI	0.050	0.000
X_7	GDP	0.030	0.000
X_8	POP	0.030	0.000
X_9	Road density	0.003	0.008
X_{10}	HAI	0.115	0.000
X_{11}	LA	0.147	0.000
X_{12}	DIVISION	0.086	0.000
X_{13}	SDI	0.110	0.000
X_{14}	MSI	0.036	0.000

Table 9 Interactive effects between the factors

	Tem	Pre	Elevation	Slope	NPP	NDVI	GDP	POP	R-density	HAI	LA	DIVISION	SDI	MSI
Tem	0.031													
Pre	0.046	0.020												
Elevation	0.069	0.077	0.067											
Slope	0.040	0.033	0.075	0.012										
NPP	0.052	0.040	0.089	0.030	0.019									
NDVI	0.120	0.113	0.167	0.072	0.059	0.050								
GDP	0.065	0.059	0.111	0.039	0.038	0.068	0.030							
POP	0.062	0.053	0.111	0.039	0.040	0.069	0.043	0.030						
R-density	0.036	0.027	0.073	0.016	0.022	0.053	0.033	0.033	0.003					
HAI	0.204	0.216	0.250	0.143	0.118	0.136	0.124	0.124	0.117	0.115				
LA	0.240	0.249	0.284	0.187	0.147	0.160	0.153	0.153	0.148	0.178	0.147			
DIVISION	0.126	0.121	0.151	0.096	0.096	0.109	0.102	0.102	0.090	0.174	0.199	0.086		
SDI	0.151	0.151	0.183	0.120	0.120	0.130	0.134	0.134	0.112	0.185	**0.205**	0.119	0.110	
MSI	0.077	0.068	0.100	0.049	0.052	0.076	0.055	0.055	0.040	0.143	0.165	0.097	0.121	0.036

Note: Yellow represents bilateral enhancement of both factors, and grey represents nonlinear enhancement.

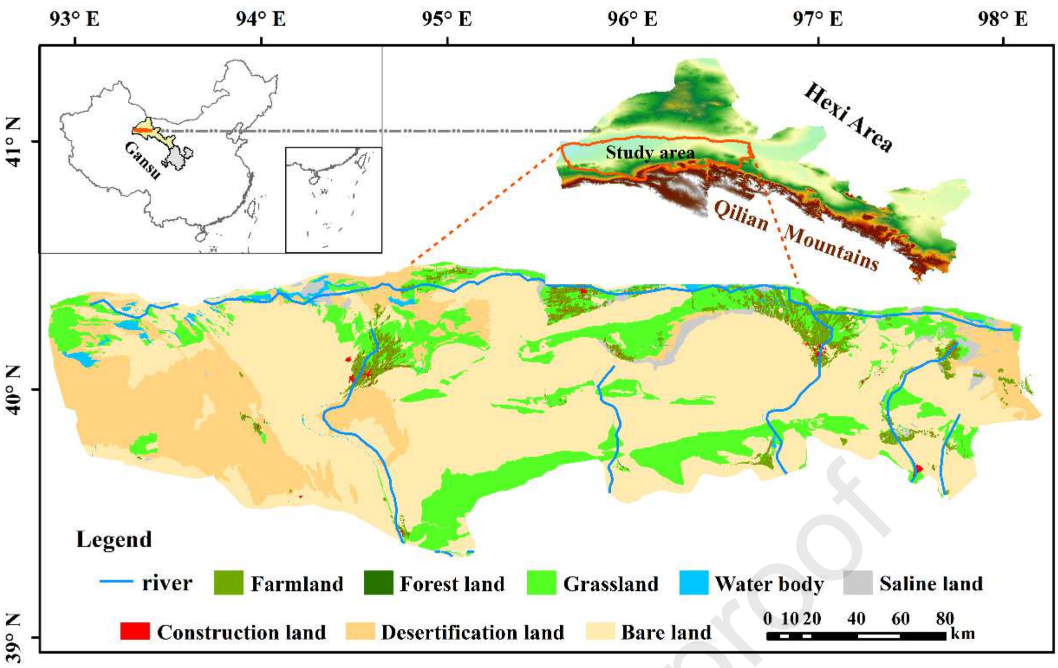

1085 Fig. 1 Location of study area.

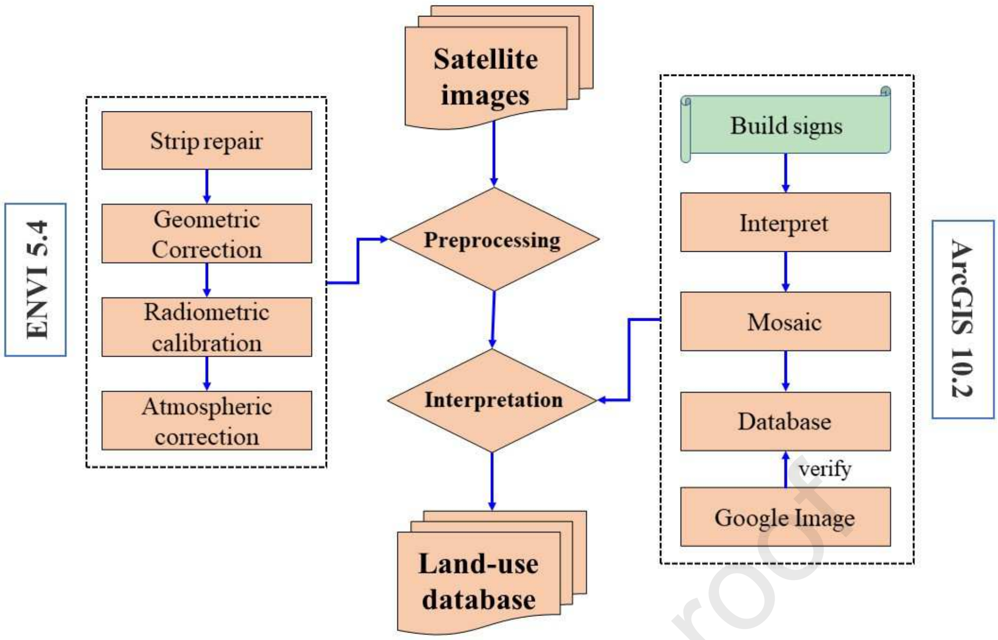

1087 Fig. 2 The establishment process of land use database in the study area.

1088

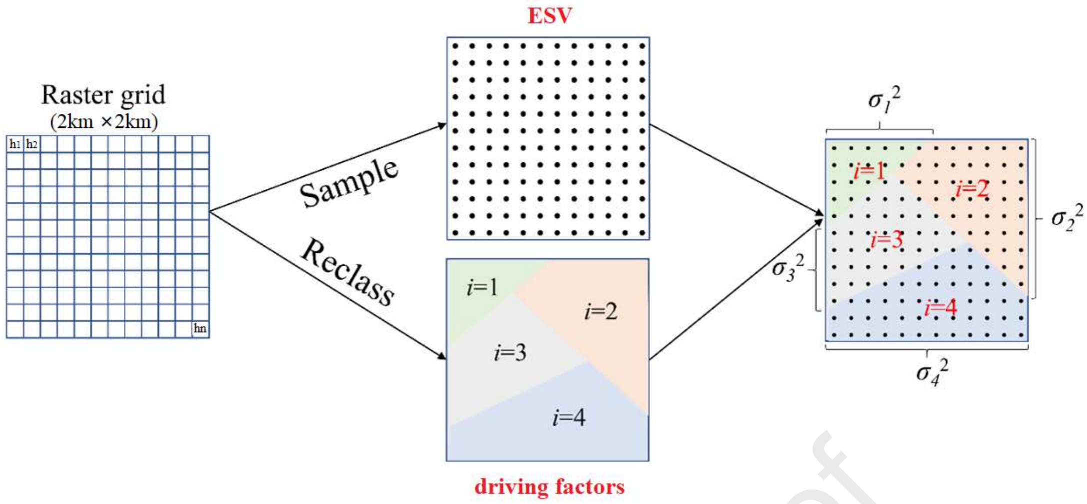

1089 Fig. 3 The principle of geographical detector models.

1090

1091
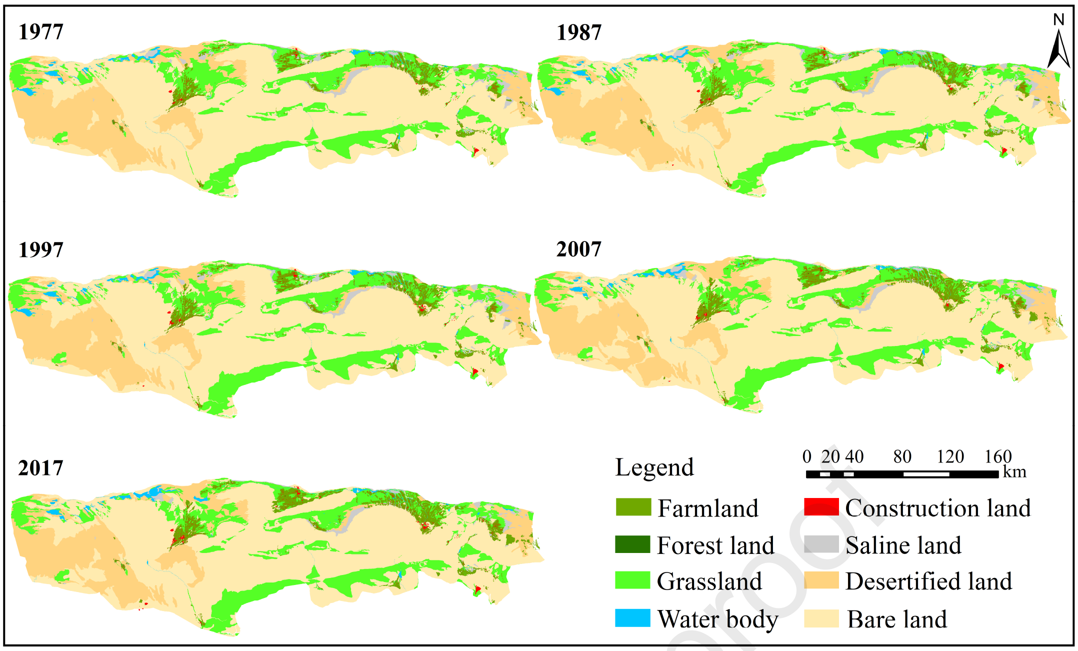

1092 Fig. 4 LULC maps of study area from 1977-2017.

1093

1094
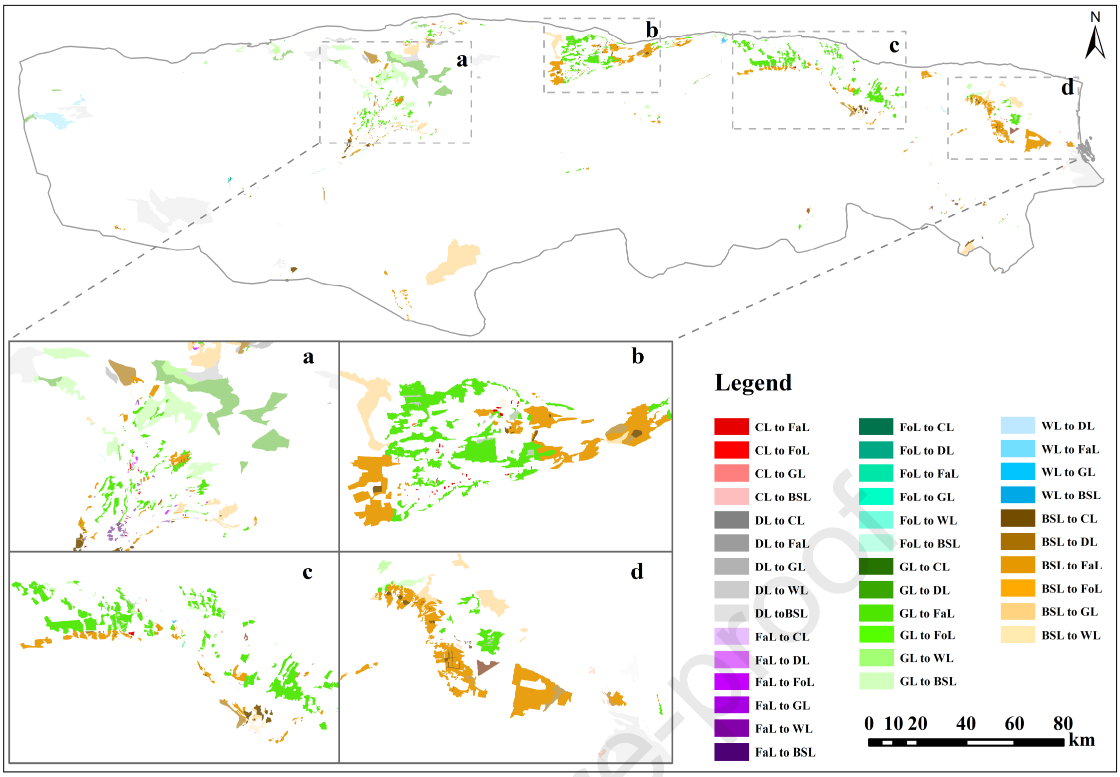

1095 Note: BSL refers to bare and saline land.

1096 Fig. 5 Spatial distribution of LULC in the study area from 1977 to 2017.

1097

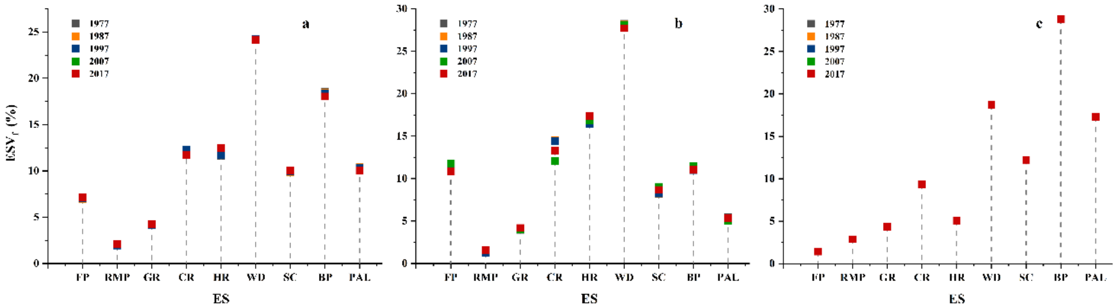

Definitions of acronyms given in Table 1.

Fig. 6 Dynamics of ESV$_f$ for study area (a), oasis system (b) and desert system (c) from 1977 to 2017. Definitions of acronyms given in Table 1.

1103 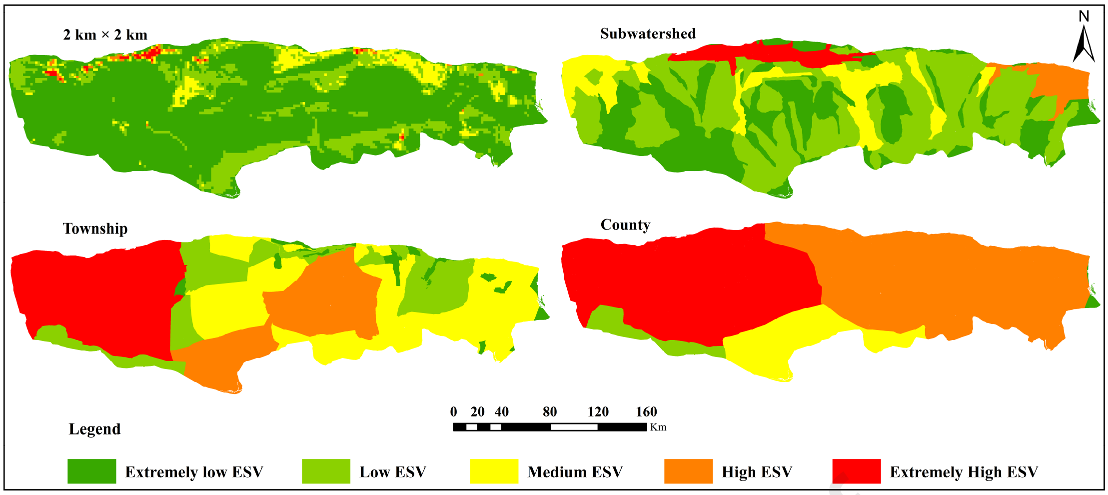

1104 Fig. 7 Spatial distribution characteristics of ESV in study area under different
1105 spatial scales.
1106

1107
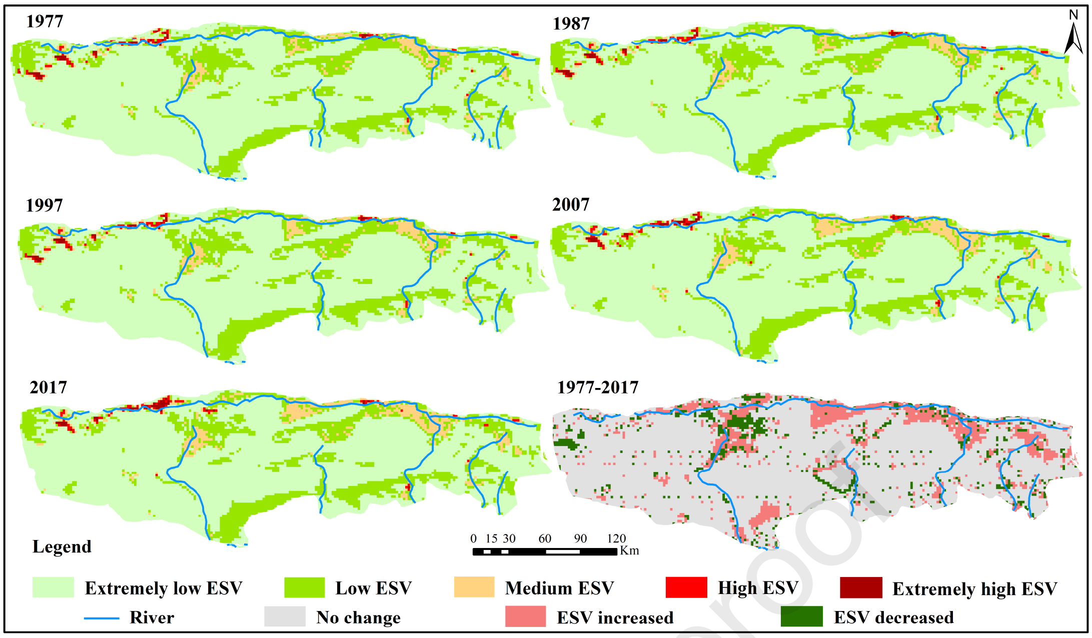

1108 Fig. 8 Spatial distribution of ESV in the MDSB.

1109

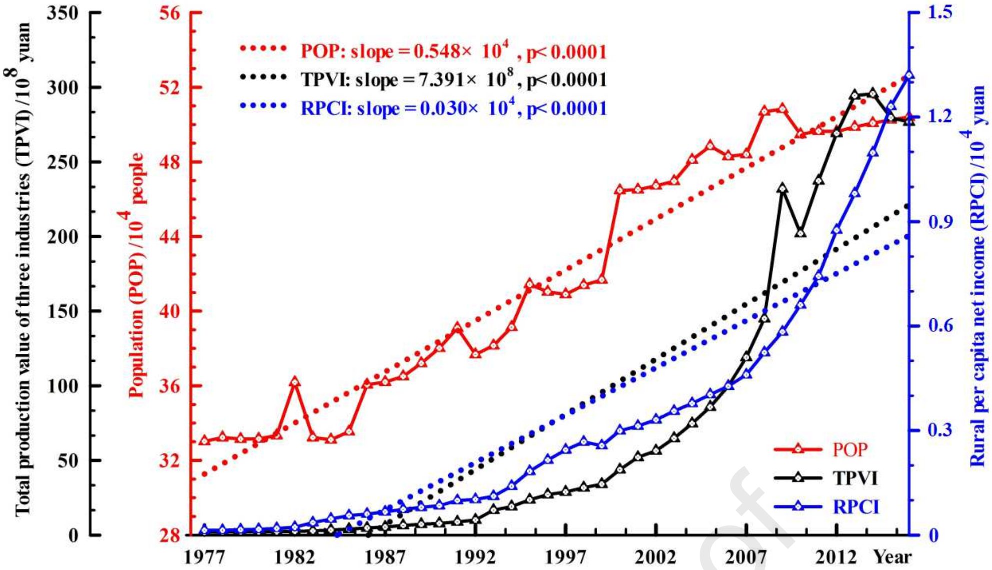

Fig. 9 Variation in total population, the total production value of 3 industries, and rural per capita net income in the MDSB.

Please find enclosed the manuscript: "**Spatial Differentiation and Driving Mechanisms in Ecosystem Service Value of Arid Region：A case study in the middle and lower reaches of Shule River Basin, NW China**", which we wish to be considered for publication in your journal. No conflict of interest exits in the submission of this manuscript, and manuscript is approved by all authors for publication. I would like to declare on behalf of my co-authors that the work described was original research that has not been published previously, and not under consideration for publication elsewhere, in whole or in part. All the authors listed have approved the manuscript that is enclosed.